VIII International Workshop on
Semiconductor Gas Sensors
11-15 September 2012, City Hotel Cracow, Poland

Tailoring of WO_3 and V_2O_5 Nanostructures for Gas Sensing Applications

Jyrki Lappalainen[1], Krisztian Kordas[1], Joni Huotari[1], Jarmo Kukkola[1], and Anita Lloyd Spetz[1,2]

[1]Microelectronics and Materials Physics Laboratories, University of Oulu, Finland
[2]Div. of Applied Sensor Science, Dept. of Physics, Chemistry and Biology, Linköping University, Sweden

University of Oulu

Founded in 1958
6 faculties
17 000 students
3 000 employees
Total funding EUR 208 million
Among the largest universities in Finland with an exceptionally wide scientific base

OULUN YLIOPISTO
UNIVERSITY of OULU

Contents:

1. WO_3 nanoparticles and thin films by PLD
   - Nanoparticle deposition
   - XRD and Raman spectroscopy results
   - SPM and SEM characterization
   - Electrical properties
   - Gas sensitivity properties

2. Inkjet printed metal decorated WO_3 nanoparticle gas sensors
   - Inkjet printing technique
   - Metal nanoparticle decoration of WO_3 nanoparticles
   - Gas sensitivity properties

3. Vanadium oxide nanostructures by PLD
   - Deposition parameters
   - XRD and Raman spectroscopy results
   - SPM and SEM characterization
   - Electrical properties
   - Gas sensitivity properties

4. Conclusions

WO_3 structure and applications:

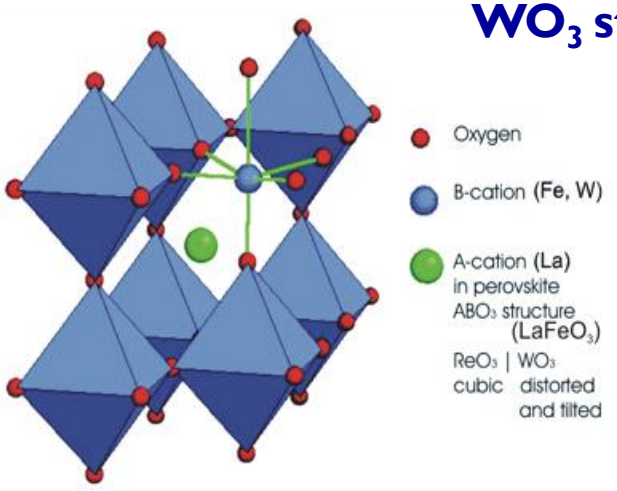

PROPERTIES OF WO_3

- Physical properties of the strcuture depend crucially on the details of the distortions and tilting of oxygen octahedra in the structure
- Electrical characteristics:
  - electrochromic (smart windows)
  - n-type semiconductor (gas sensing)
  - ferroelectric in ε-WO_3 phase in nanocrystals @ RT

Different phases of WO_3 (crystal structures)*

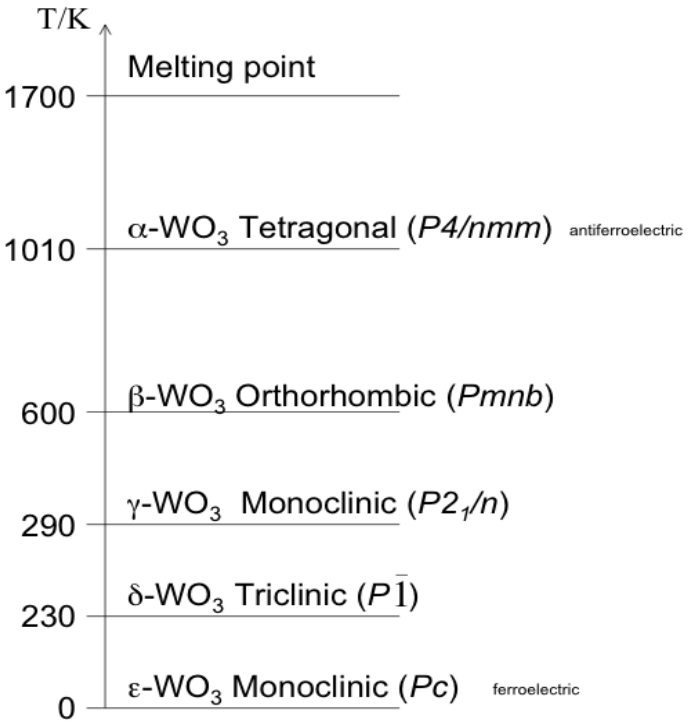

*P. M. Woodward, A. W. Sleight, and T. Vogt. Ferroelectric tungsten trioxide. *Journal of Solid State Chemistry*, 131(1):9-17, 1997.

PLD of WO_3 thin films and nanoparticles:

- WO_3 nanoparticle growth by PLD:
  - Low partial gas pressure → normal growth of WO_3 thin film
  - Increase in partial gas pressure → decrease in growth rate, change in growth mode
  - Point where nanoparticulate formation starts → **growth of ε-WO_3 phase nanoparticles**

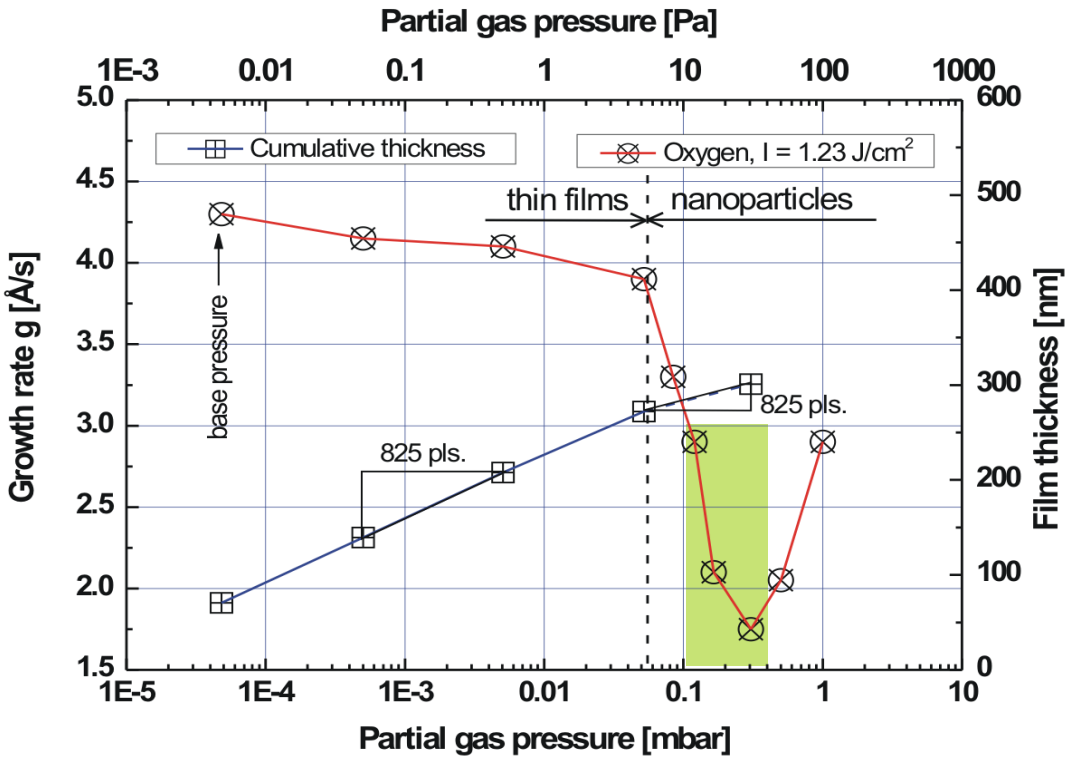

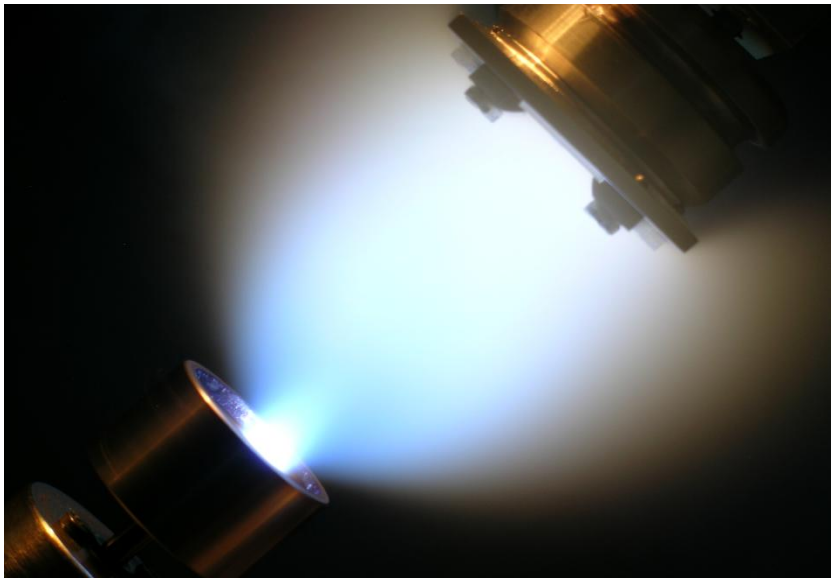

Results – XRD:

- WO_3 structural characterization by XRD:
  - Clear crystalline WO_3 responses observed even in *ex situ* deposited samples
  - Due to small particle size and thin films, XRD analysis of phase structure is complicated
  - Main phase of *in situ* deposited samples was monoclinic γ-WO_3 RT-phase

(a) ex situ (RT) deposited WO_3:

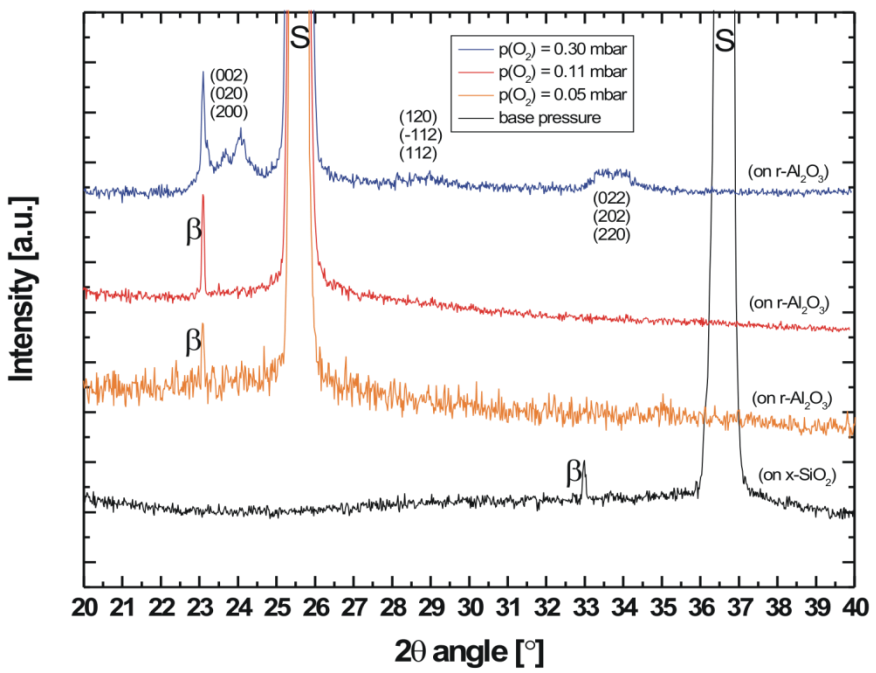

(b) effect of different heat-treatments:

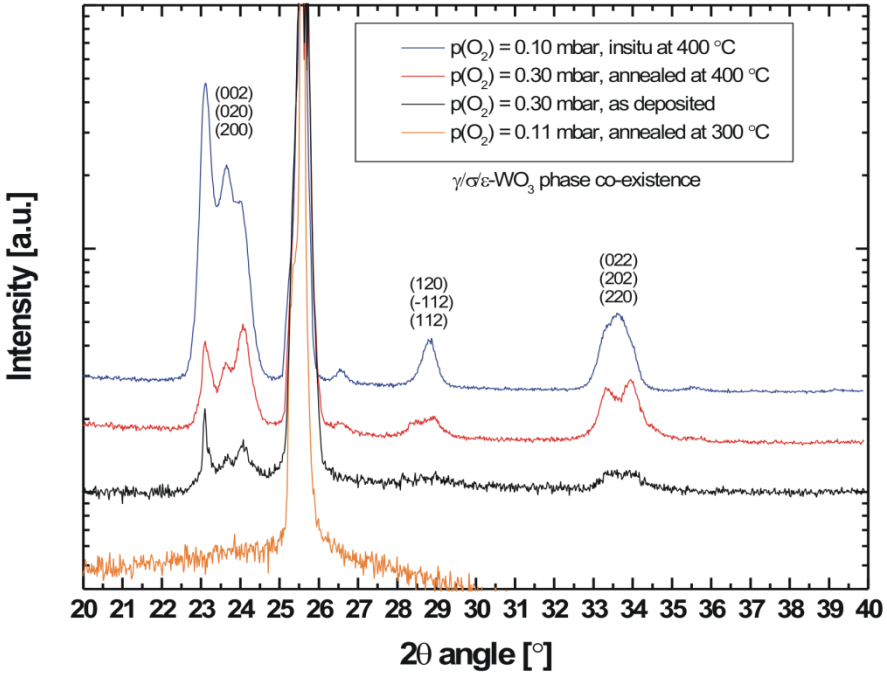

Results - Raman spectroscopy:

- WO_3 structural characterization by Raman spectroscopy:
  - Clear crystalline WO_3 Raman modes observed even in *ex situ* deposited samples
  - ε-WO_3 phase Raman modes measured at RT when $p(O_2)$

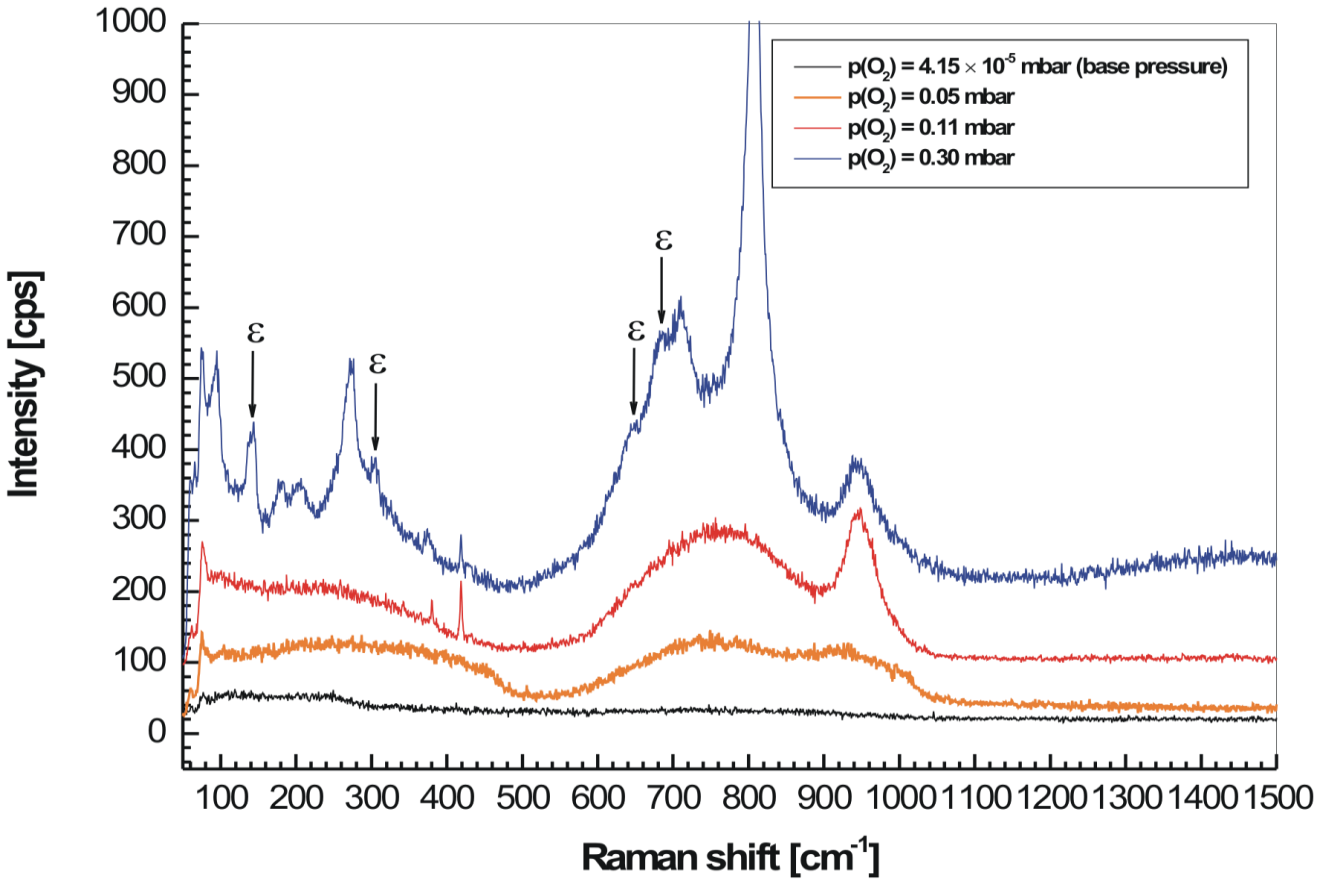

Results - Raman spectroscopy:

- WO_3 structural characterization by Raman spectroscopy:
  - ε-WO_3 phase Raman modes are enhanced after 30 min post-annealing treatment at 400 °C

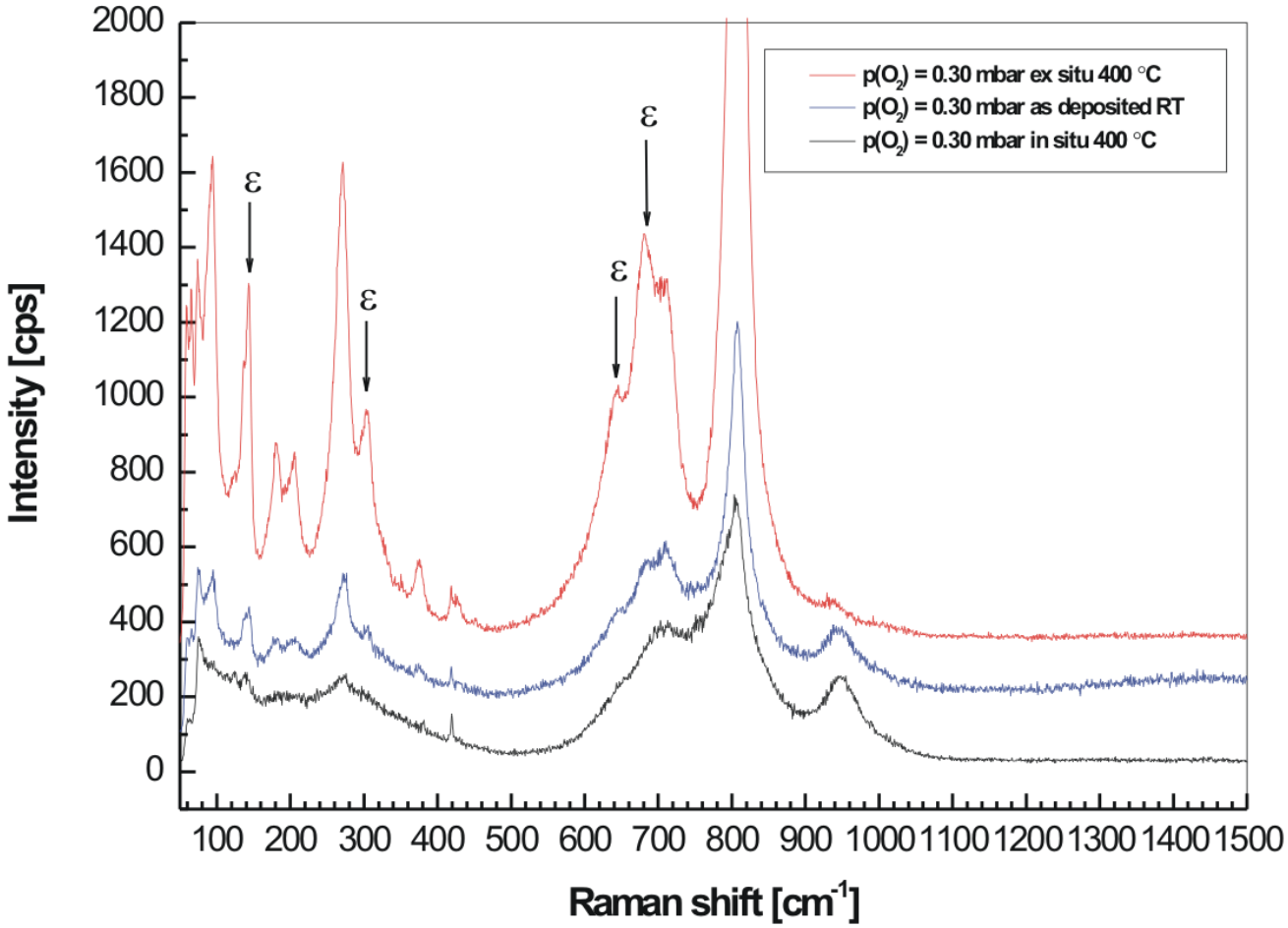

SPM and SEM characterization:

- WO_3 structural characterization by SPM:
  - Surface morphology (R_q) developeded from very flat thin film to porous nano-particle or -agglomerate structure with increasing $p(O_2)$

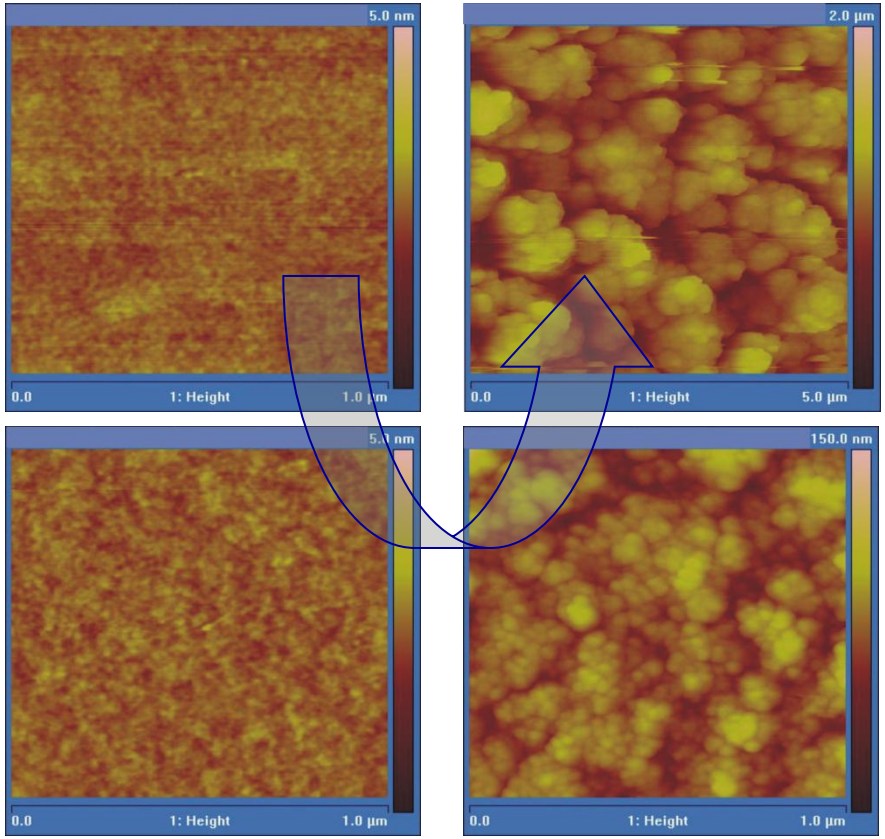

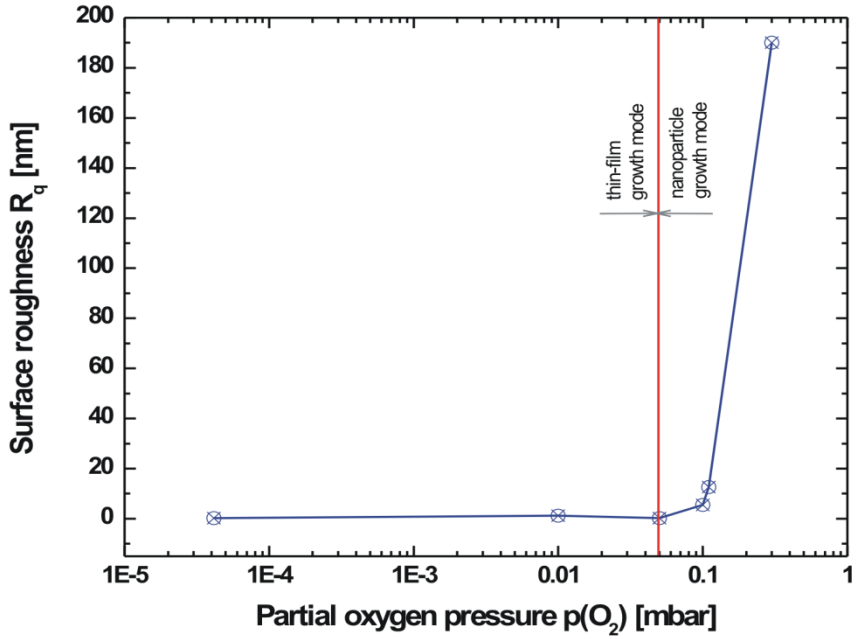

Microstructure studies of WO_3 -nanoparticle thin films:

b3.7 - $p(O_2)$=0.05 mbar

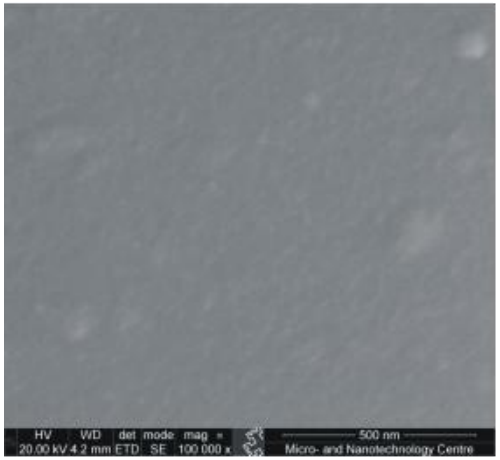

b3.8 - $p(O_2)$=0.08 mbar

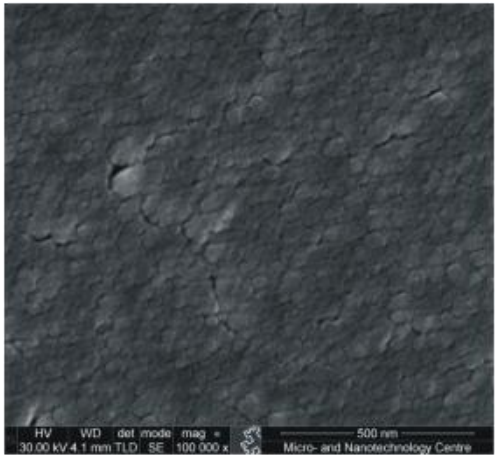

b3.9 - $p(O_2)$=0.1 mbar

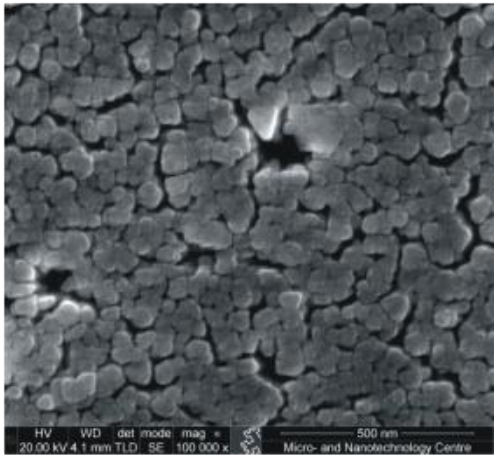

b3.10 - $p(O_2)$=0.2 mbar

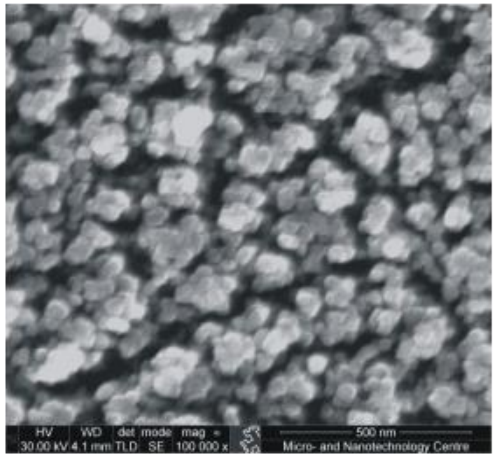

b3.5 - $p(O_2)$=0.3 mbar

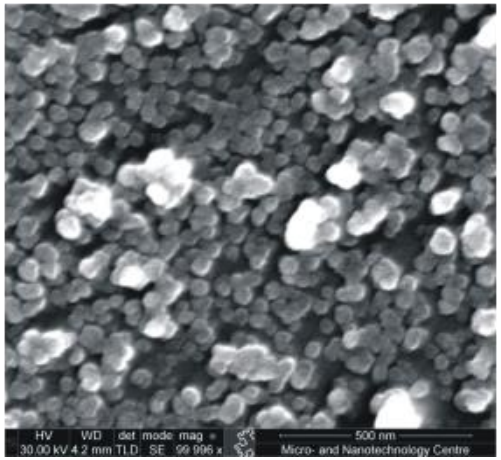

b3.5 - $p(O_2)$=0.5 mbar

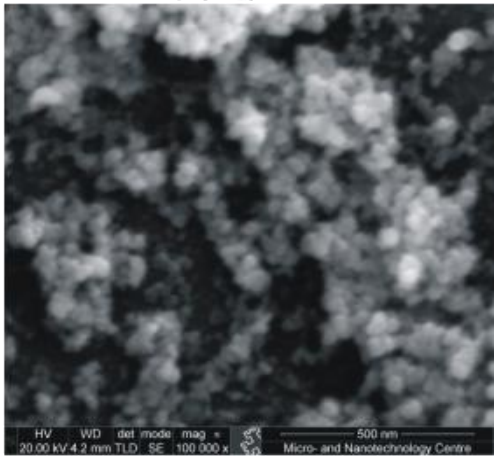

SPM and SEM characterization:

- WO_3 structural characterization by SEM:
  - according to SEM and Warren-Averbach analysis on XRD data, the mean grain size of the nanocrystalline *ex situ* films varied from 30 to 50 nm.

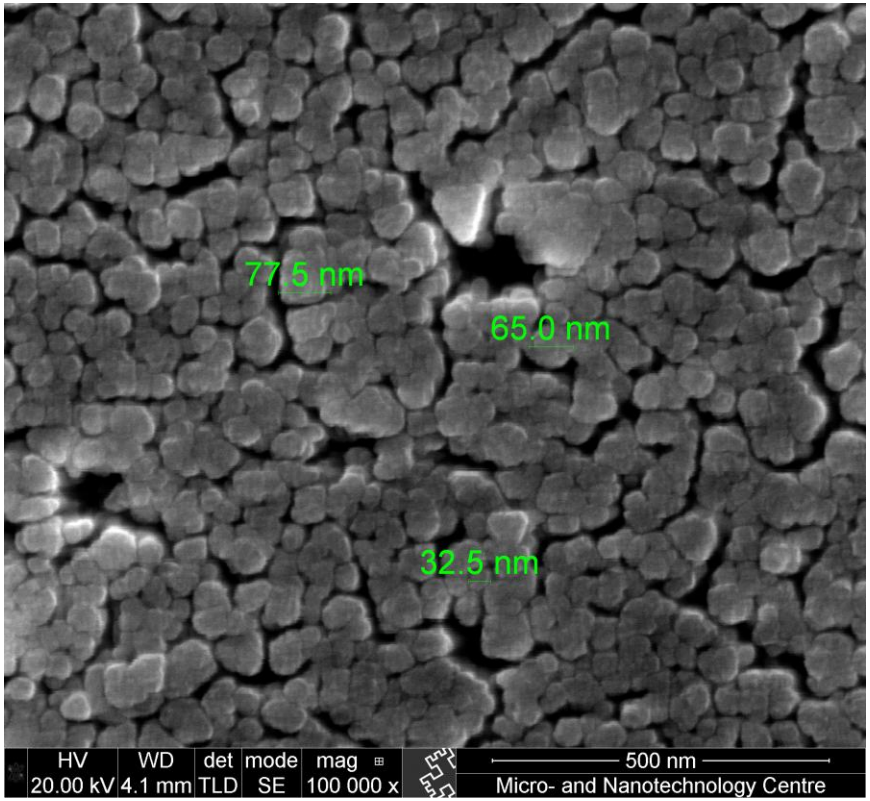

In situ: $T_s \approx 400$ °C, $p(O_2) = 0.1$ mbar

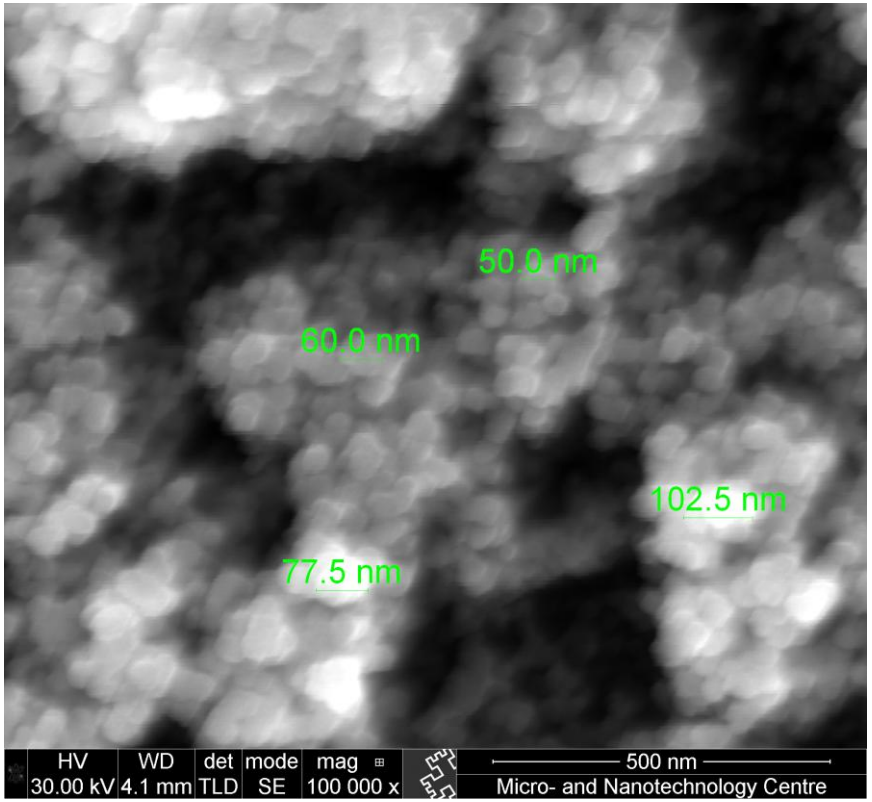

Ex situ: $T_s \approx$ RT, $p(O_2) = 0.3$ mbar

Results - Dielectric properties:

- Dielectric constant $\varepsilon_r(T,f)$ and loss angle $\tan\delta(T,f)$ response showed an dielectric anomaly typical for ferroelectric materials at $T_c \approx 200$ °C!
- In order to confirm real ferroelectricity, more research is required. Other, for example, space charge and surface reaction effects are also possible.

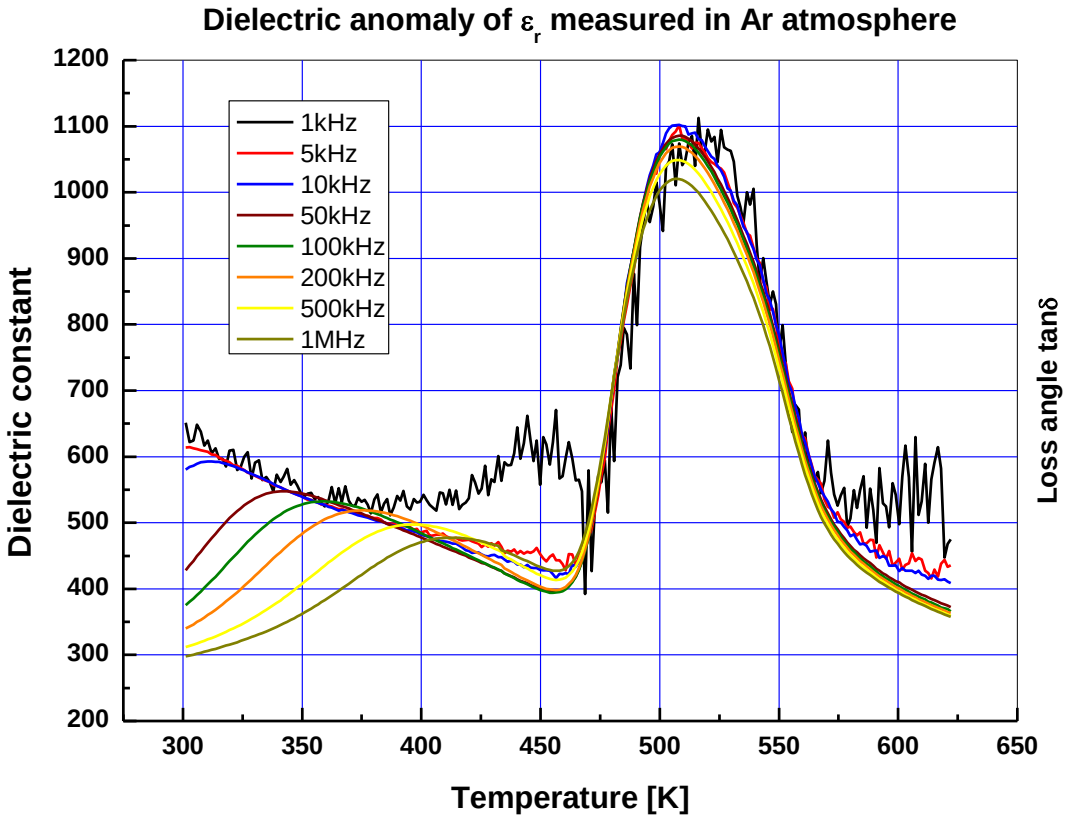

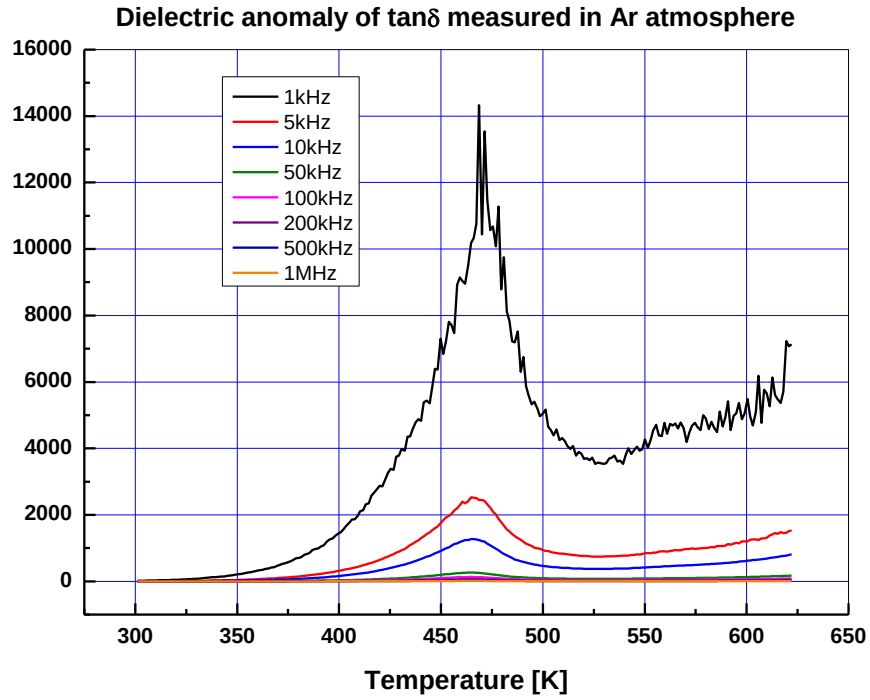

Results - Gas sensitivity properties:

- H_2S response from 1 to 195 ppm in synthetic air at 200 °C. Cleaning at 350 °C.

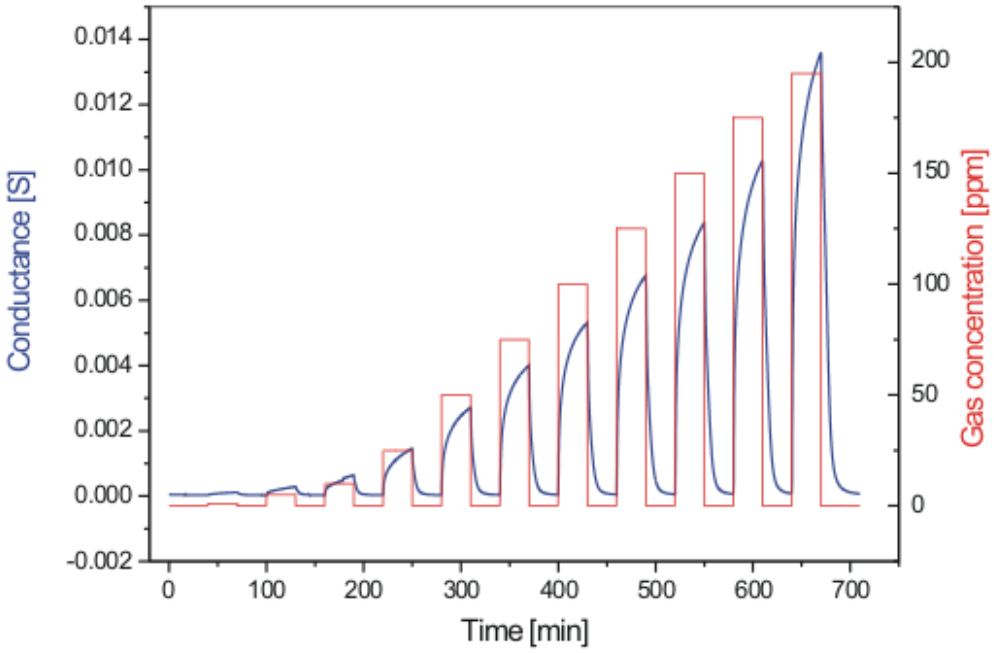

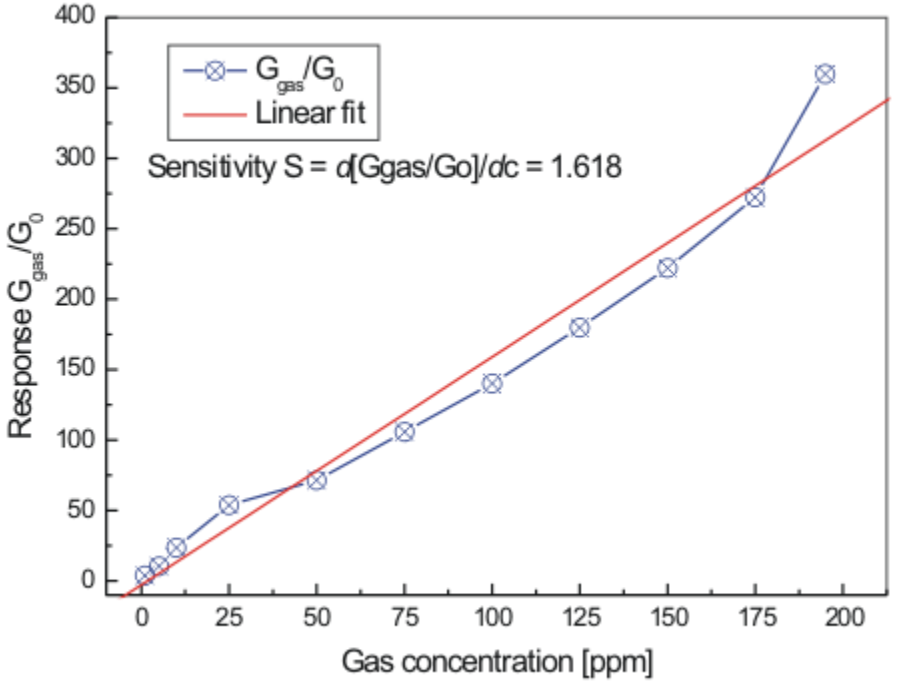

Results - Gas sensitivity properties:

- H_2 response from 5 to 100 ppm in synthetic air at 200 °C. Cleaning at 350 °C.

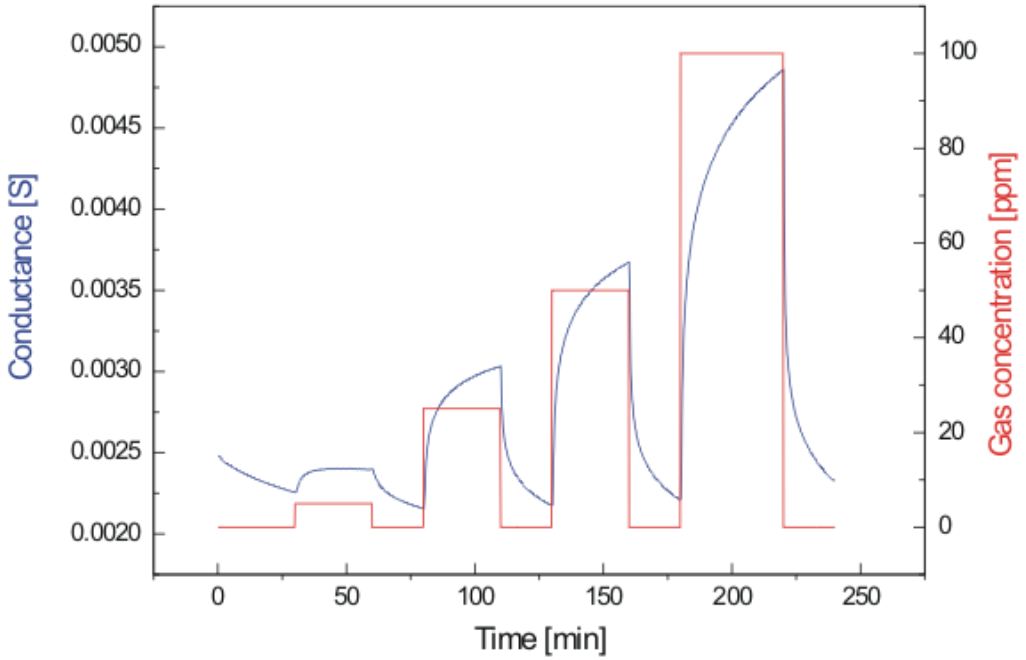

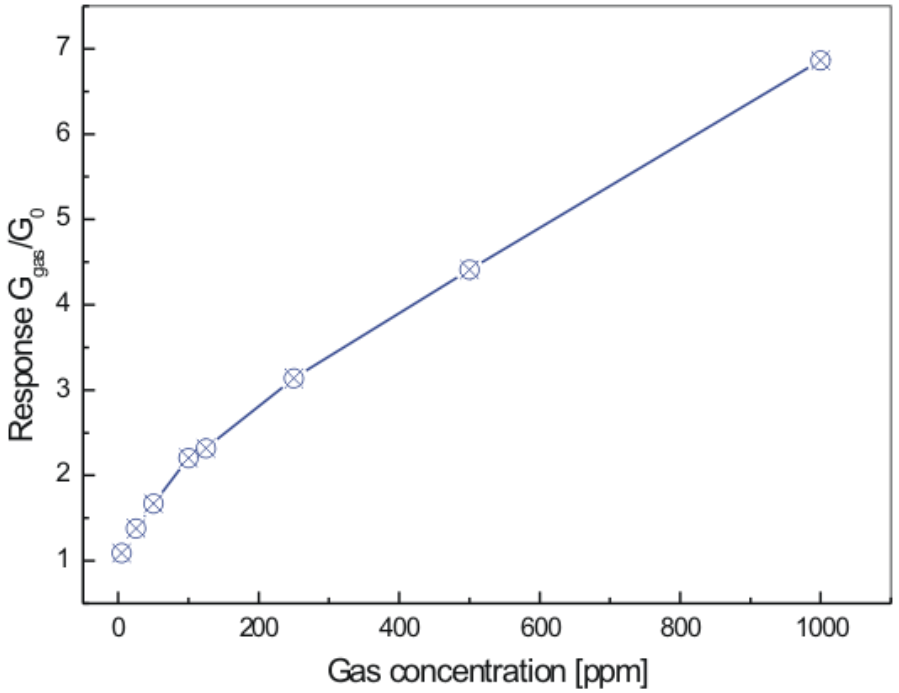

Results - Gas sensitivity properties:

• CO response from 10 to 1000 ppm in synthetic air measured at several temperatures. Cleaning at 350 °C.

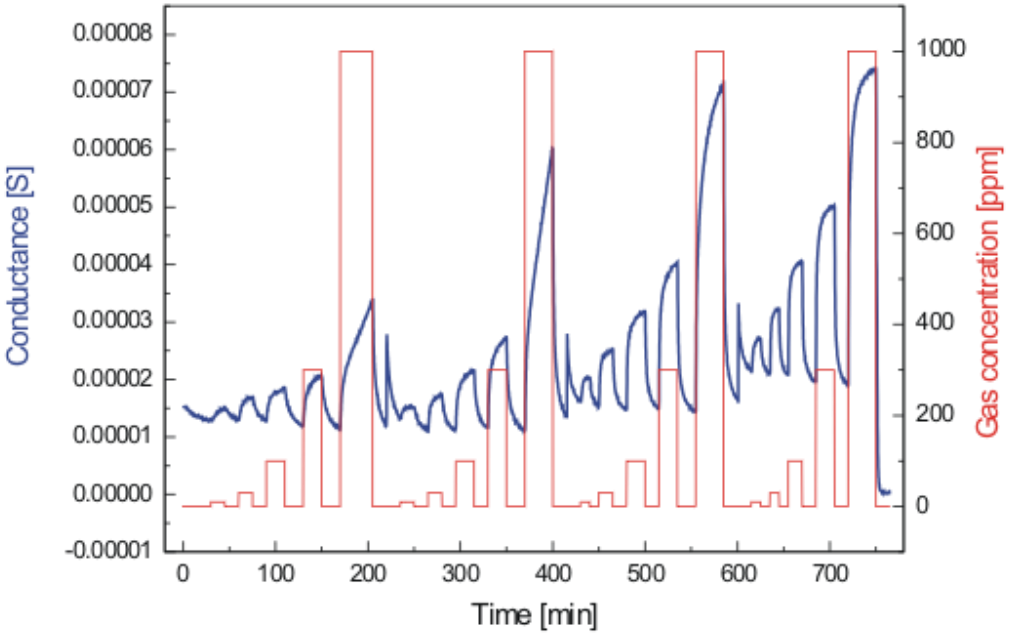

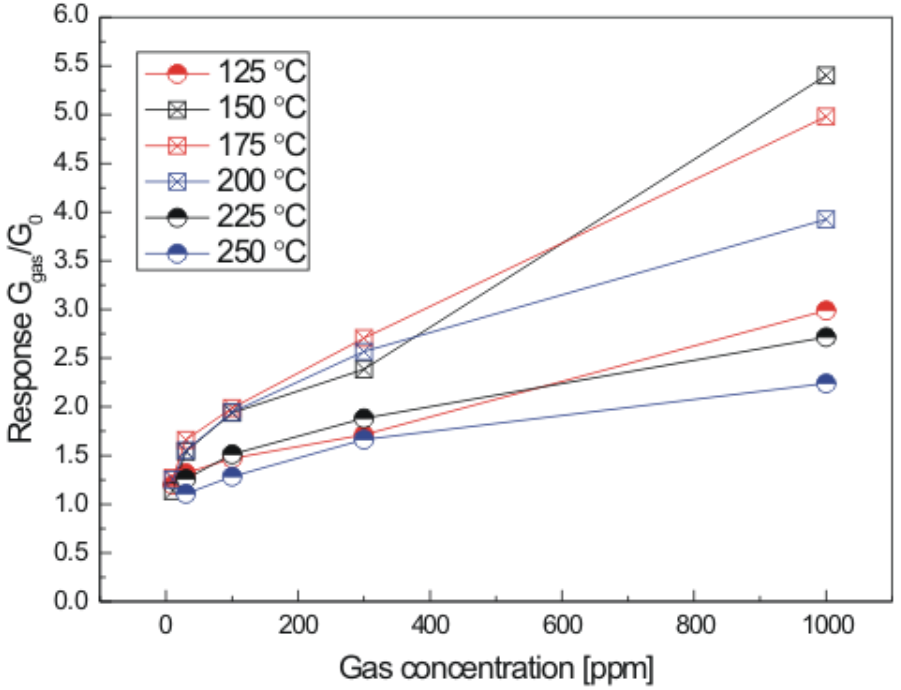

Results - Gas sensitivity properties:

- NO_x response from 5 to 90 ppm in synthetic air measured at several temperatures. Both reducing and oxidizing gas responses! Cleaning at 350 °C.

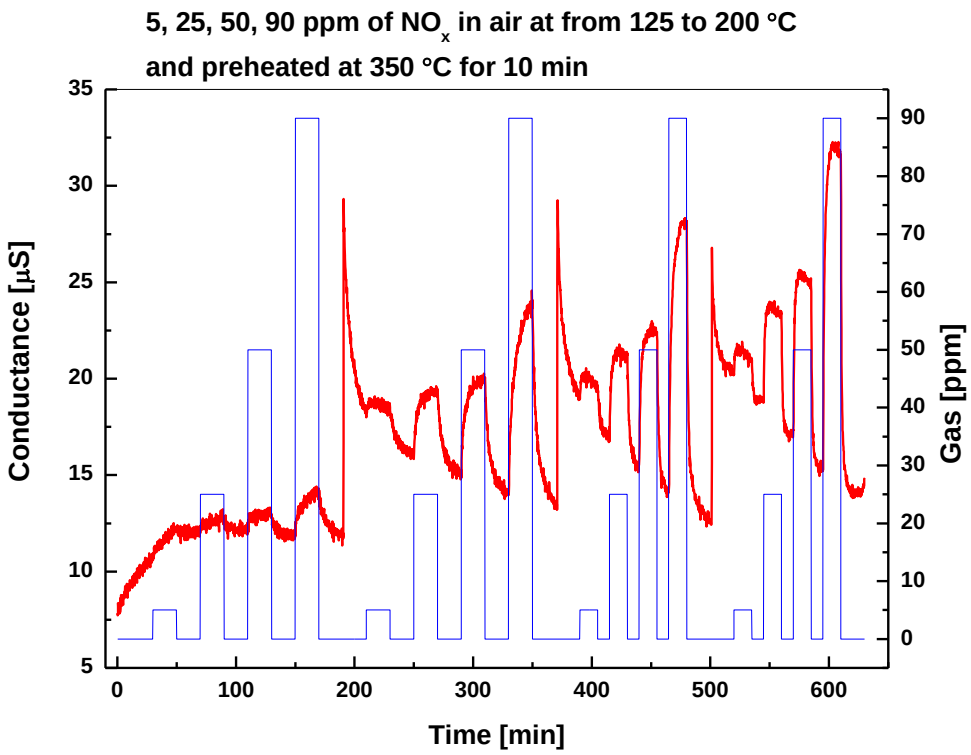

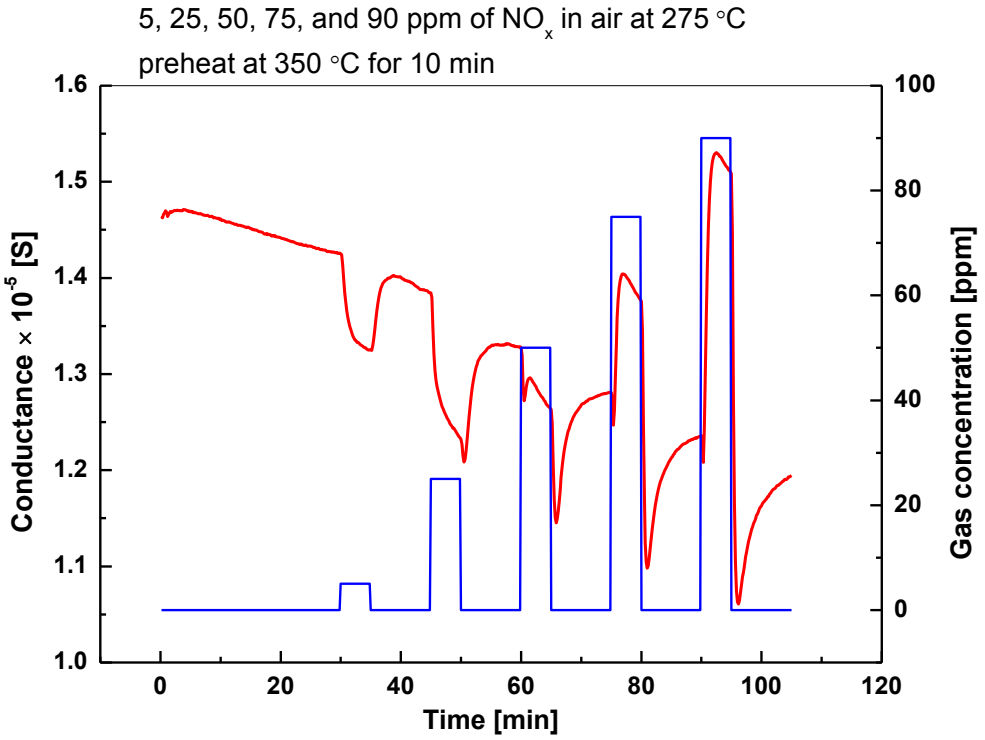

WO_3 -nanoparticle sensor response for NO_x:

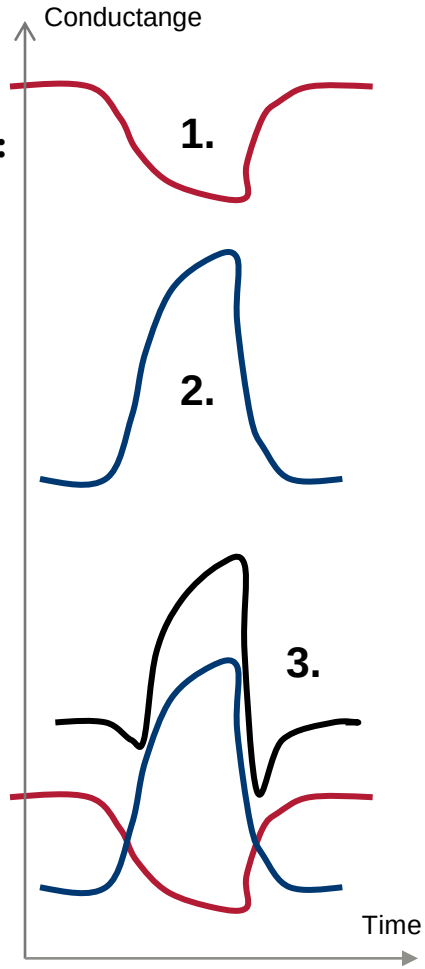

1. Oxidizing process:
$X^{n+} + ne^- \Rightarrow X$

2. Reducing process:
$X^{n+} + ne^- \Leftarrow X$

3. Oxidizing and reducing processes combined!

If one considers a sensor heated up to temperature T, what are the reactions taking place on WO_3 thin film surface? Reasonable assumption is that reactions take place only at the surface contact between gas atmosphere and sensor surface.

Suggested reactions could be:

1. First reaction on clean surface:

$$NO(g)+2e^- \Rightarrow \tfrac{1}{2}\, N_2(g) + O^{2-}$$

$N_2(g)$ is removed from the surface (inert gas)

at low temperatures O^{2-} is adsorped, at higher T desorped

2. Second reaction on oxygen O^{2-} contaminated surface:

$$2NO(g)+O^{2-} \Rightarrow 2\, NO_2(g) + ne^-$$

$NO_2(g)$ is removed from the surface or reacts futher reaction 2 takes only place with short delay after reaction 1 at lower temperatures surface might be contaminated by oxygen from water, etc.

WO_3 -nanoparticle sensor response for NO_x:

If these reactions are responsible for the observed NO_x reaponse of WO_3 thin films and nanoparticles, the controlling factor of the process is actually the ratio of adsorption rate ν_O and desorption rate ν_{-O} of the contaminating oxygen O^{2-} ions on the surface. Both of these measures are dependent, for example, on pressure p, surface coverage θ, activation energies E_a and E_d, and temperature T:

Adsorption = sticks to surface: Desorption = leaves the surface:

$$\nu_O = \frac{\sigma p}{\sqrt{2\pi m k T}} f(\Theta) \exp\left[\frac{-E_a}{kT}\right], \quad \nu_{-O} = k_{-O} f_{-O}(\Theta) \exp\left[\frac{-E_d}{kT}\right]$$

$\Rightarrow$ when $\nu_O > \nu_{-O}$ the response is dominated by reduction process (2)!

$\Rightarrow$ when $\nu_O < \nu_{-O}$ the response is dominated by oxidizing process (1)!

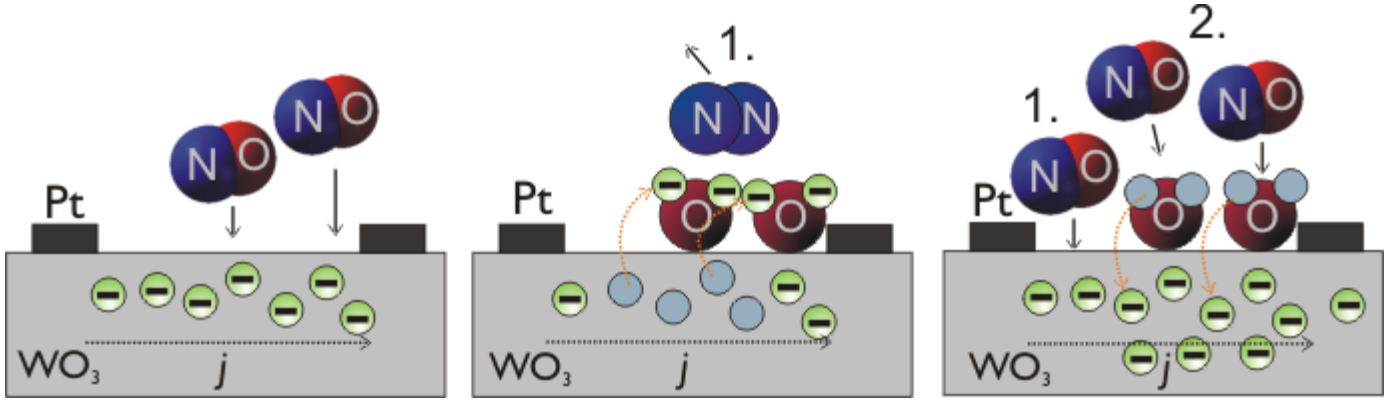

$$j = \sigma E = n\mu e E \quad \Rightarrow \quad \Delta j \propto \Delta\sigma \propto \Delta n$$

WO_3 -nanoparticle sensor response for NO_x:

Gas sensitivity properties - NO_x response in air of WO_3 depends on the dissociation process of oxygen on the sensor surface, and is thus both temperature and concentration dependent!

Needs further research!

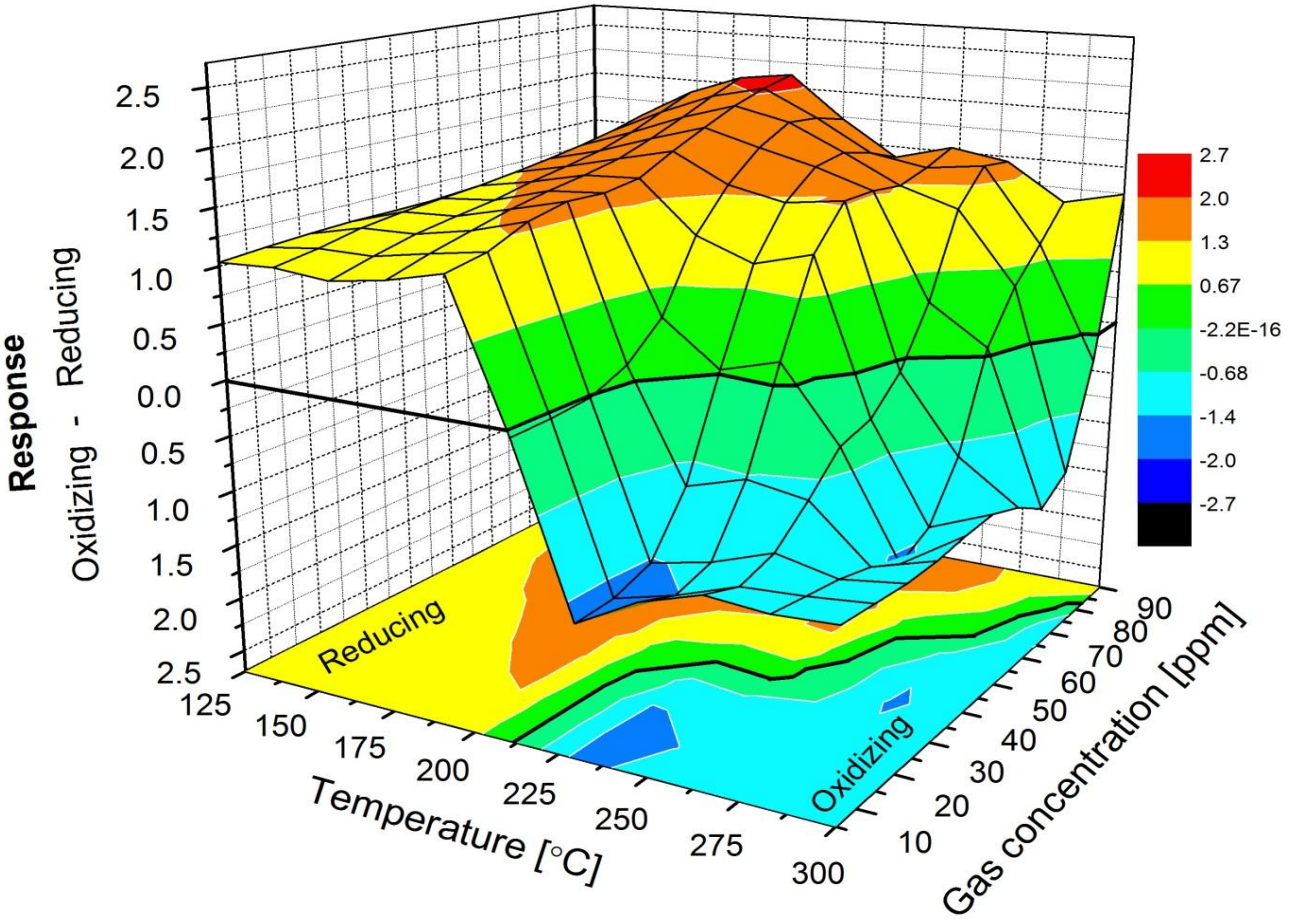

Contents:

Printing techniques for gas sensor fabrication:

Printing technologies have a great potential to be utilized in electronic manufacturing.

Requires understanding of material chemistry and printing expertise.

Printing methods

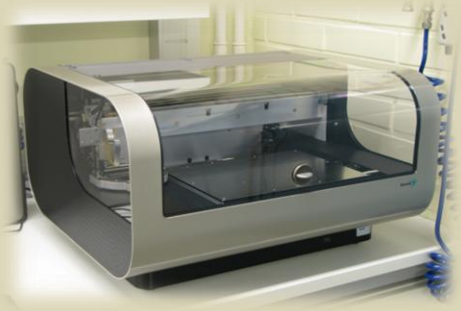

Inkjet-printer

Gravure printer

Principle of printing methods

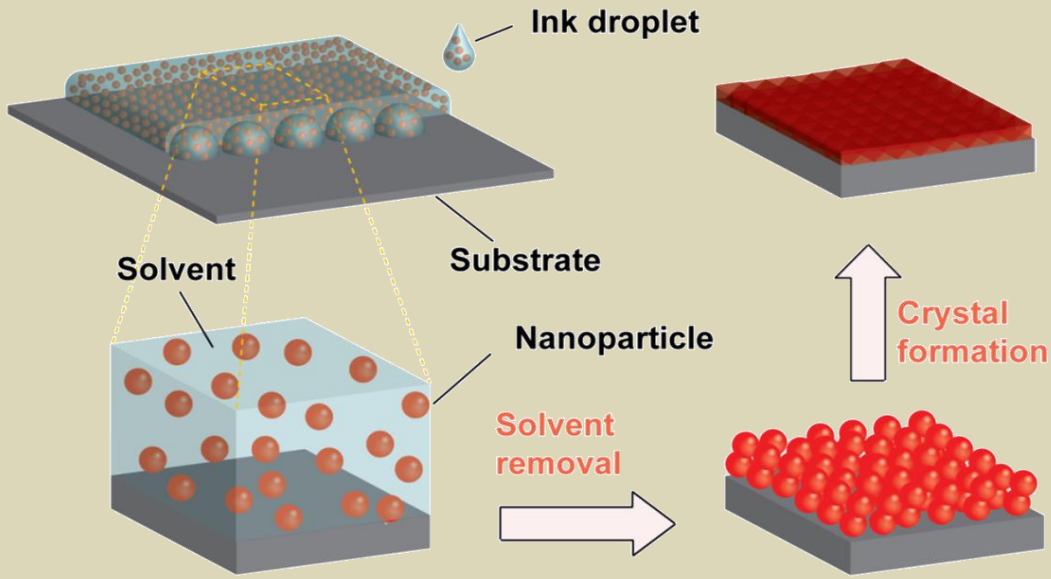

Decoration of WO_3 NPs with metal(oxide) NPs:

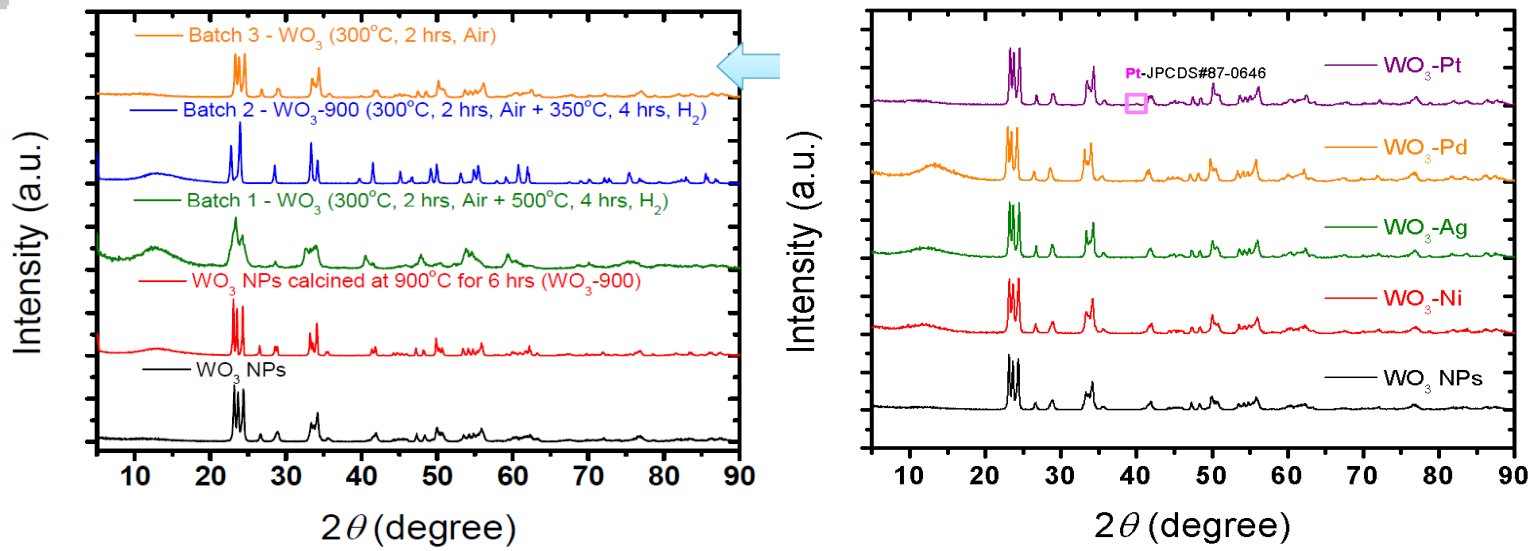

According to XPS and EDX there is 1-4 % of metal nanoparticles mixed with WO_3 nanoparticles.

WO_3-Ni/NiO WO_3-Ag/Ag_2O WO_3-Pd/PdO WO_3-Pt

1. Nickel (II) Acetylacetonate
2. Silver Nitrate
3. Palladium (II) Acetylacetonate
4. Platinum (II) Acetylacetonate

Calcined at 300˚C for 2 hours in air

Decoration of WO_3 NPs with metal(oxide) NPs:

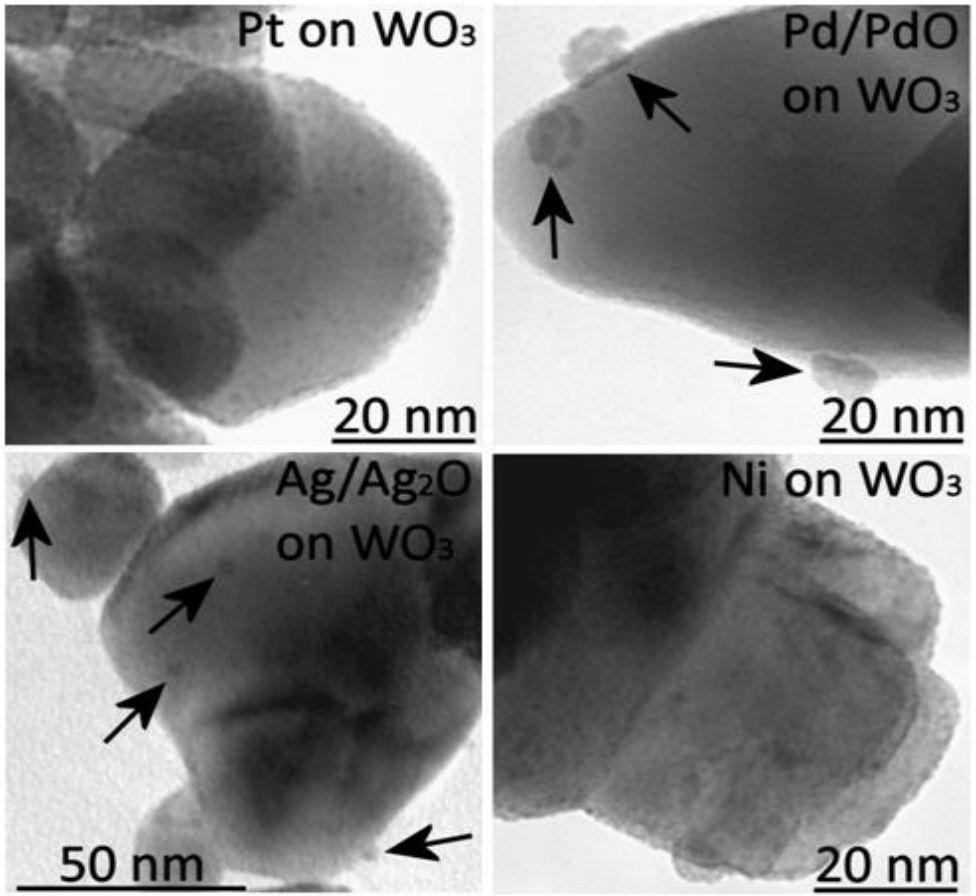

Catalyst prec.	Size, TEM	Conc., XPS	Conc., EDX	Ox. St. XPS
$AgNO_3$	~4 nm	0.6 wt.%	0.6 wt.%	Ag(0)
$Ni(acac)_2$	~1 nm	4.1 wt.%	2.6 wt.%	Ni(II)
$Pd(acac)_2$	~4 nm	2.3 wt.%	0.7 wt.%	Pd(II)
$Pt(acac)_2$	~1 nm	3.6 wt.%	0.9 wt.%	Pt(0),(II),(IV)

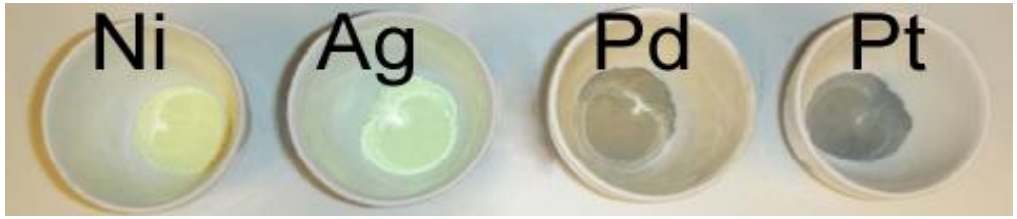

XPS analysis of decorated WO_3 NPs:

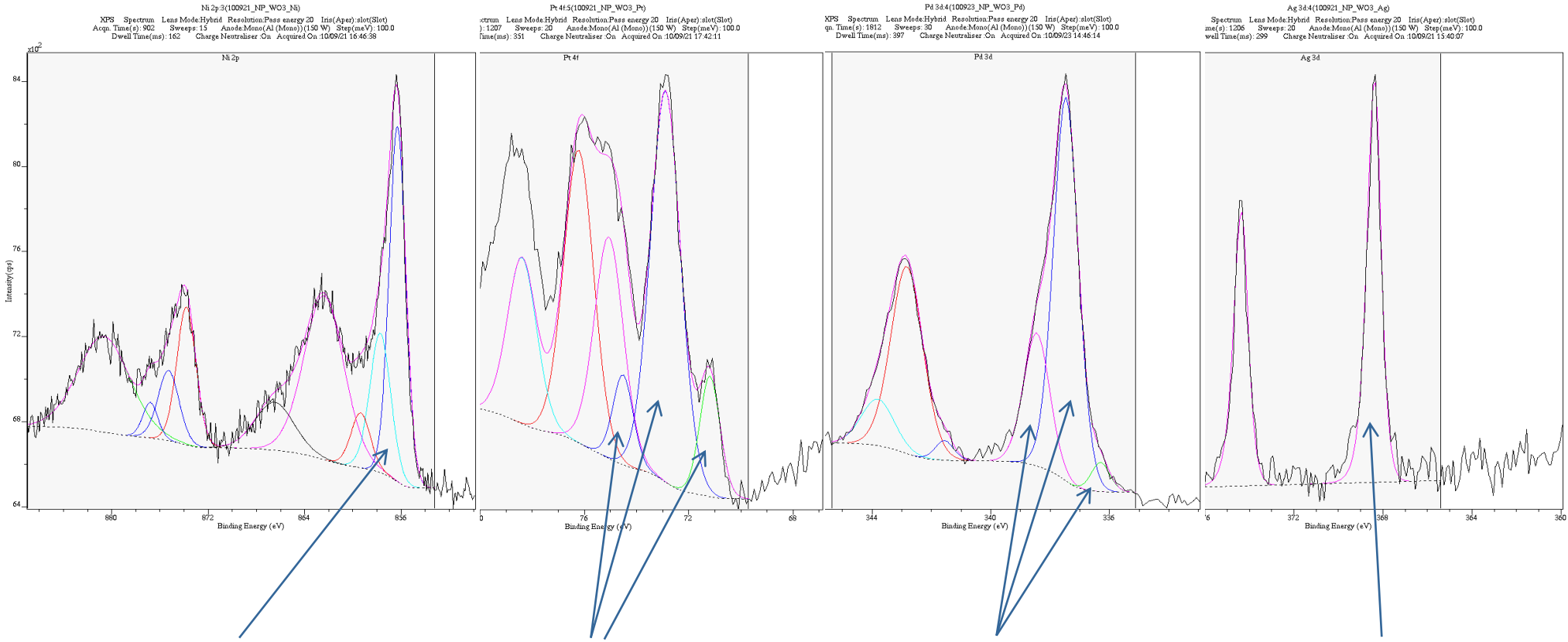

Ni 2p 3/2 at 856.3 eV
Ni(II)

Pt 4f 7/2 at
71.2; 72.9; 75.1 eV
Pt, Pt(II), Pt(IV)

Pd 4d 5/2 at
336.3; 337.5; 338.5 eV
Pd (II), Pd(IV)

Ag 3d 5/2
368.4 eV
Ag

Inkjet Printed Metal Decorated Tungsten Oxide Nanoparticles for Gas Sensing:

- **Printing of WO_3 nanoparticle inks**
- The inks were printed between Pt electrodes on Si/SiO_2 chips:
  - -20 layers of 200 µm long lines with 20 µm drop spacing
    - ~2 nanograms per sensor of WO_3 NPs
      - The cost of WO_3 NPs per million sensors is 1.5 cents (0.015 euros)
      - Printing of one sensor takes 6 minutes (could be optimized with industrial printers)

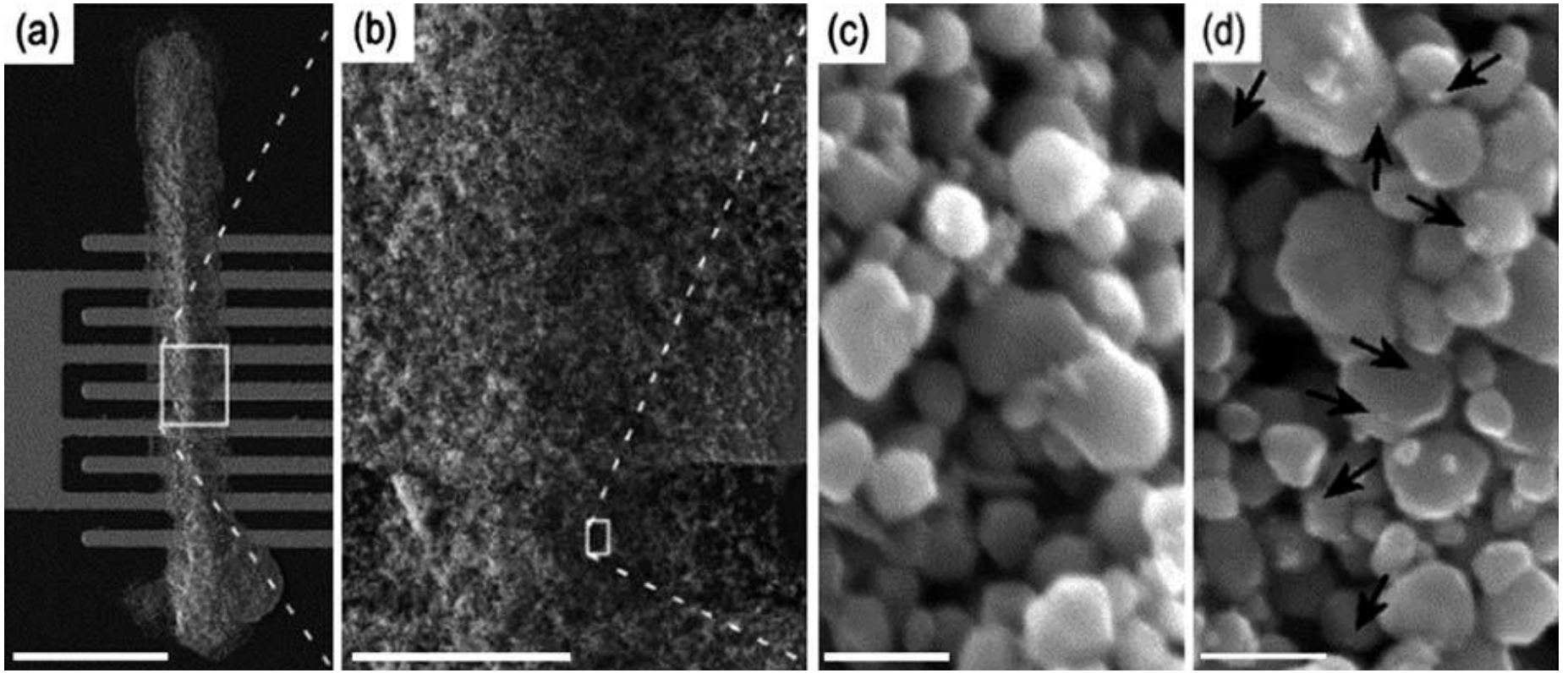

Gas sensing with semiconducting metal oxide nanoparticles - Inkjet printed resistive WO_3 nanoparticle gas sensors:

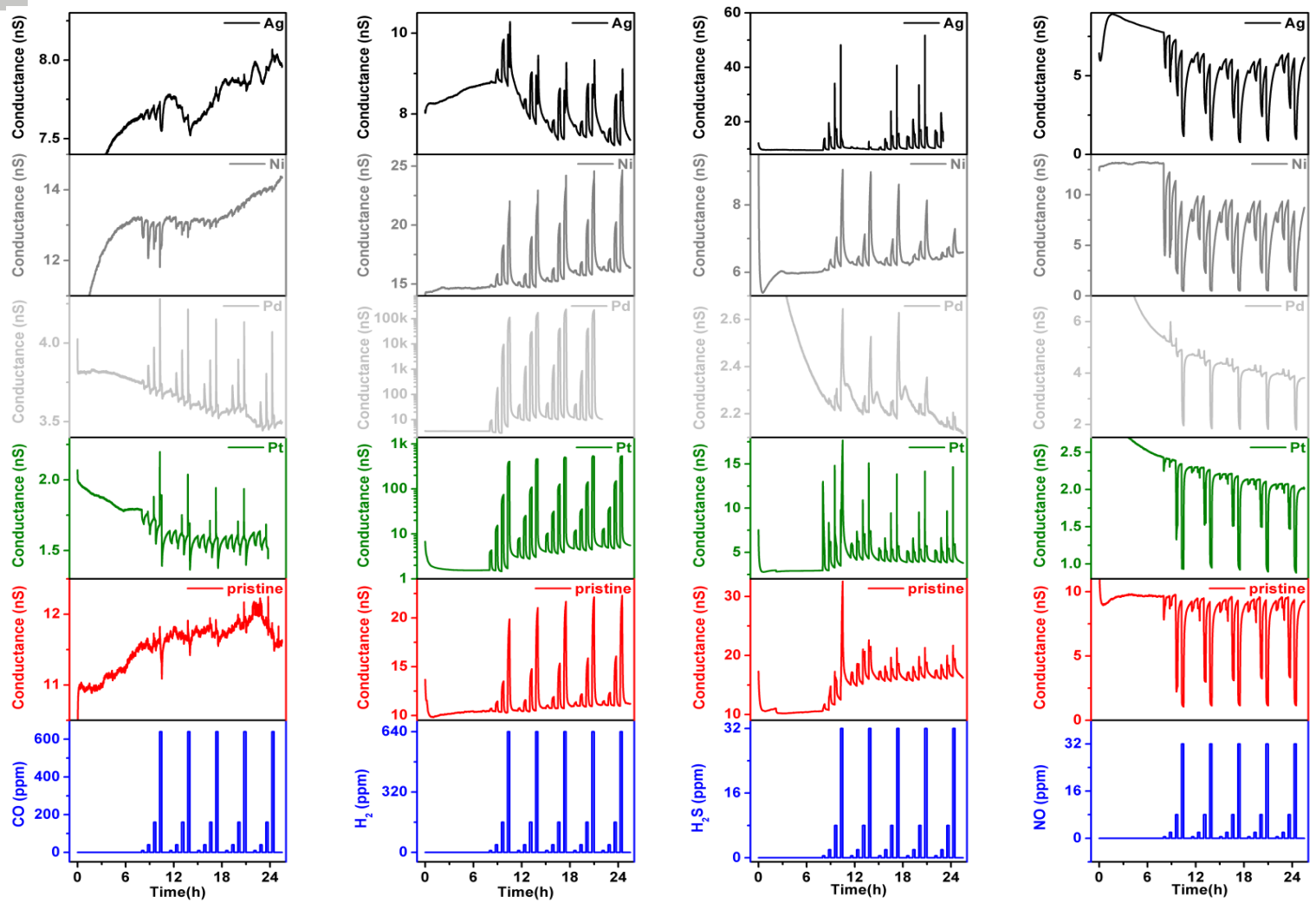

WO_3 nanoparticles decorated with metal nanoparticles and then dispersed in water for inkjet deposition (on Si chips).

Small metal(oxide) NPs:
Ag/Ag_2O of ~4 nm
Ni/NiO of ~1 nm
Pd/PdO of ~4 nm (agglomerating)
Pt of ~1 nm

In many cases, the first gas pulses were observed to have higher responses compared to the following pulses.

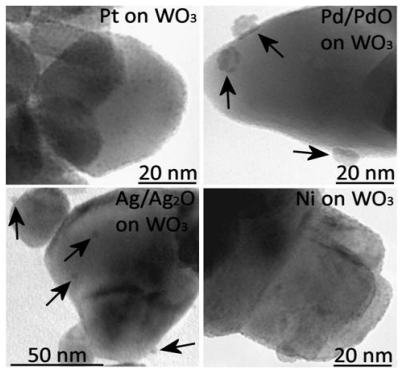

(J.Mater.Chem. 22 (2012) 17878)

Gravure printing - Nanostructure fabrication of a gas sensor:

Resistive type NO_x sensor – WO_3 nanoparticle ink:

Simple resistive type of test component is used to evaluate the suitability of WO_3 nanoparticles for gas sensor applications.

Ink composition: WO_3 nanoparticles, polystyrene binder and Triton-X 100 surfactant in toluene. Gravure printing (Schläfli Labratester) onto Ag finger (litography, 50 nm) electrodes on PEN. After treatment:
Drying: 200 ° C, 2 h

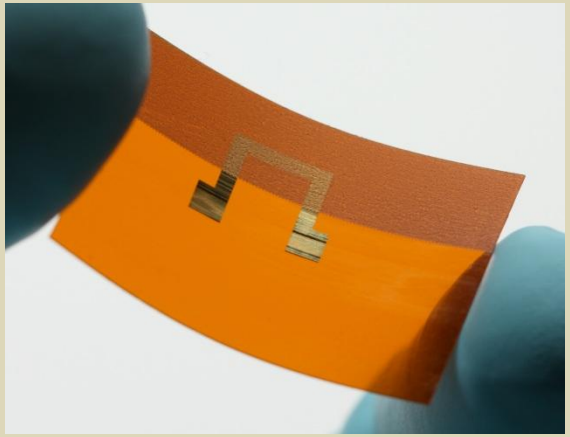

Response for NO_x at 175 °C temperature.

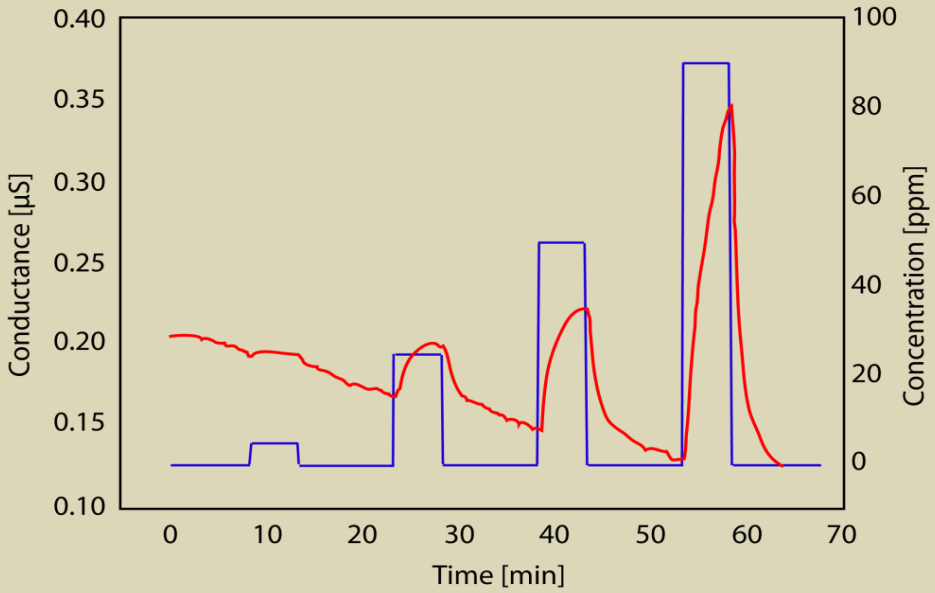

Contents:

1. WO_3 nanoparticles and thin films by PLD
   - Nanoparticle deposition
   - XRD and Raman spectroscopy results
   - SPM and SEM characterization
   - Electrical properties
   - Gas sensitivity properties

2. Inkjet printed metal decorated WO_3 nanoparticle gas sensors
   - Inkjet printing technique
   - Metal nanoparticle decoration of WO_3 nanoparticles
   - Gas sensitivity properties

3. Vanadium oxide nanostructures by PLD
   - Deposition parameters
   - XRD and Raman spectroscopy results
   - SPM and SEM characterization
   - Electrical properties
   - Gas sensitivity properties

4. Conclusions

Background:

- Semiconducting metal oxide based gas sensors is still a strong research topic in the field of gas sensing.
- Vanadium oxides (VO_2, V_2O_5 etc.) are one potential candidates for gas sensing.
- Polycrystalline vanadium oxide thin films have been shown to have sensitivity towards NO_x *(e.g. Rella et al.)*.
- Nanostructures of different vanadium oxides are studied as possible ammonia (NH_3) sensors *(e.g. Modaferri et al.)*.
- The metal-insulator transition of VO_2 is studied to find a new type of gas sensors *(e.g. Byon et al.)*.
- Here we present some new research of vanadium oxides as gas sensors.

Pulsed Laser Deposition of VO_x Thin Films:

- Pulsed laser deposition with different deposition parameters were used to manufacture vanadium oxide thin films on 1x1 cm Al_2O_3 substrates from a V_2O_5 target:

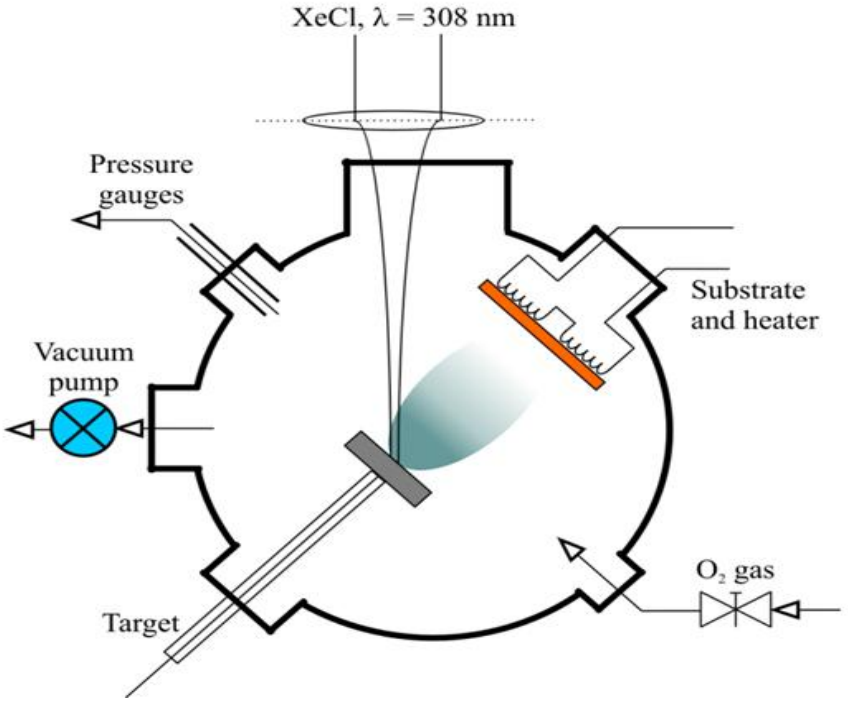

Thin film	Substrate temperature T / ° C	Oxygen partial pressure $p(O_2)$/ mbar	Laser pulse energy density I/ J/cm²
A)*	400	$1.0x10^{-2}$	1.275
B)	400	$1.5x10^{-2}$	2.55
C)	500	$1.5x10^{-2}$	2.55

* Film A) was found to be amorphous after the deposition and was post annealed in an oven at 400 °C for 1h.

Results – XRD:

- Film A) (post annealed) was a polycrystalline V_2O_5 thin film with a major (001) orientation.
- An amorphous phase was also present in film A).
- Films B) and C) showed a decrease of V_2O_5 phase.

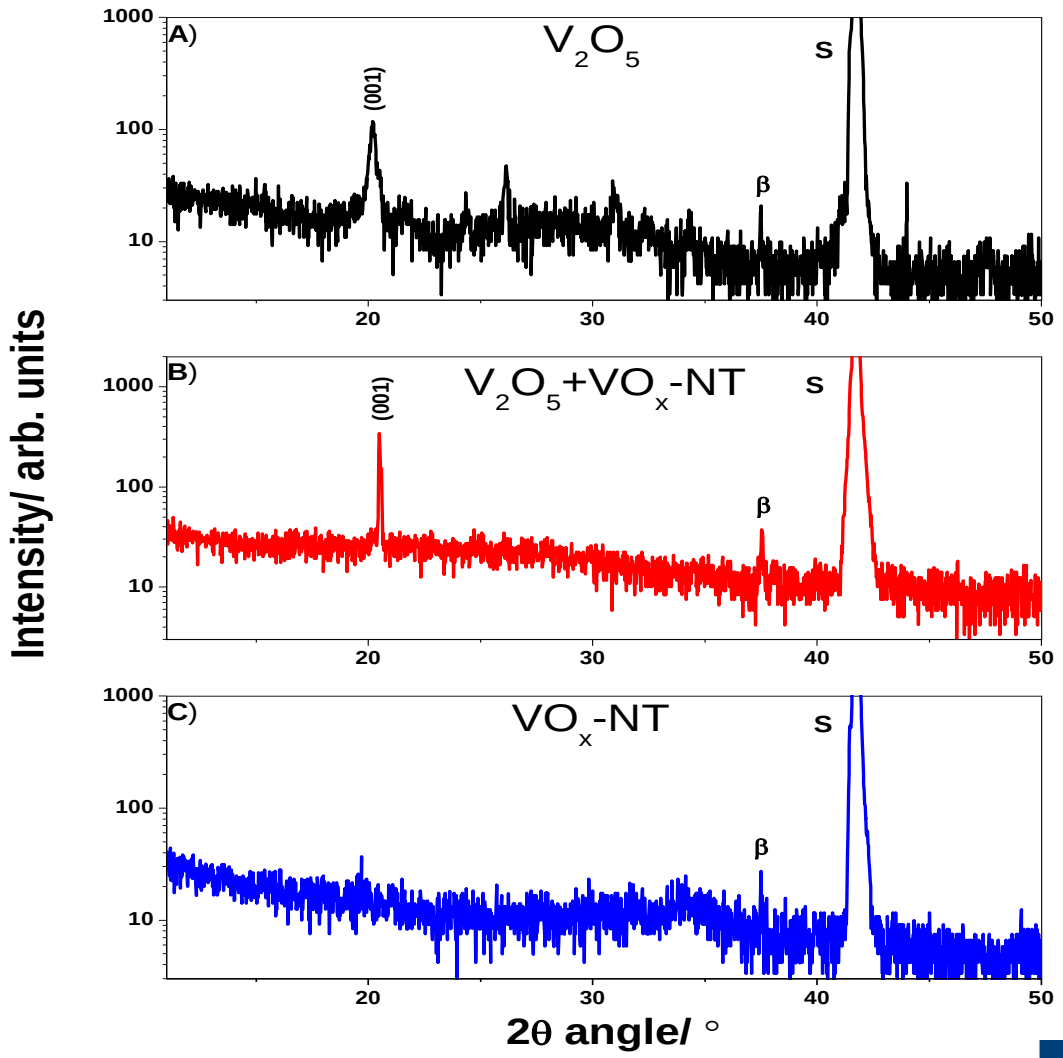

Results - Raman spectroscopy:

- Film A) showed a clear Raman spectrum of V_2O_5 phase.
- In film B) the V_2O_5 phase got weaker and some new peaks appeared (marked with black circles).
- In film C) the new peaks were dominating over the V_2O_5 phase.

⇨ The new peaks are similar to those found in vanadium oxide nanotubes (VO_x-NT) formed from layers of V_7O_{16} phase! [1,2,3]

⇨ Films had same crystal symmetry as VO_x-NT:s!

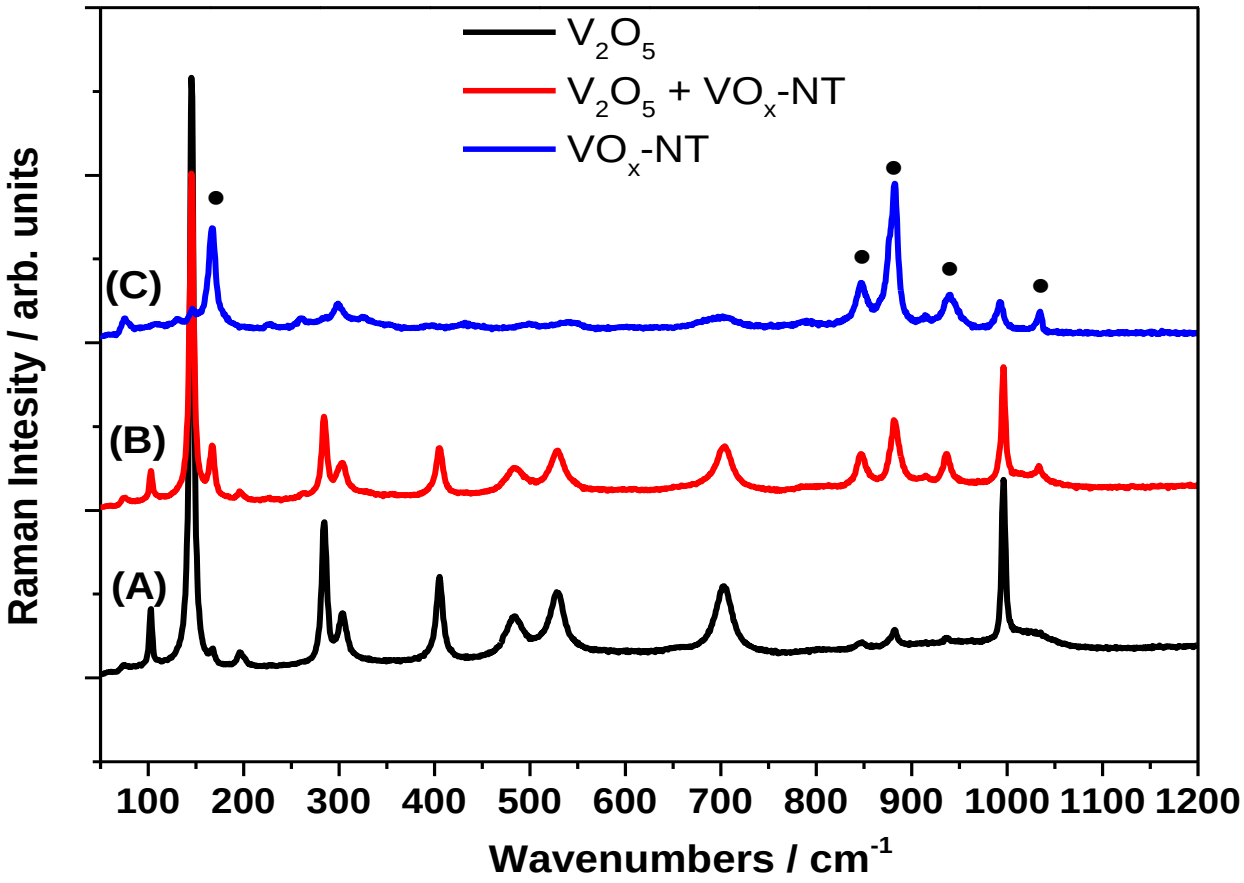

[1] Liu et al., Applied Surface Science 253, 2747-2751, (2006)
[2] Souza Filho et al., Nano Letters 4, 2099-2104, (2004)
[3] Wörle et al., Z. anorg. allg. Chem. 628, 2778–2784, (2002)

SPM and SEM characterization:

V_2O_5

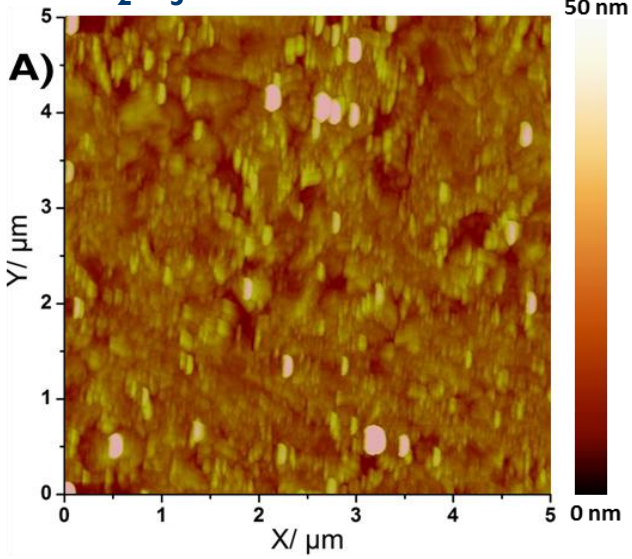

$V_2O_5 + VO_x$-NT

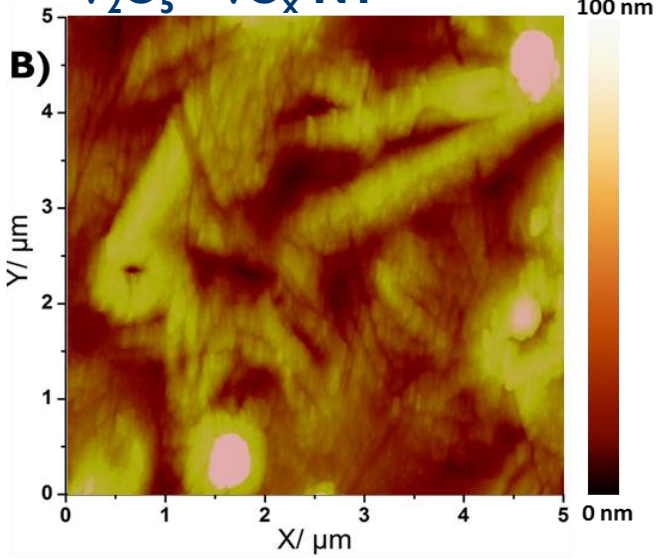

VO_x-NT

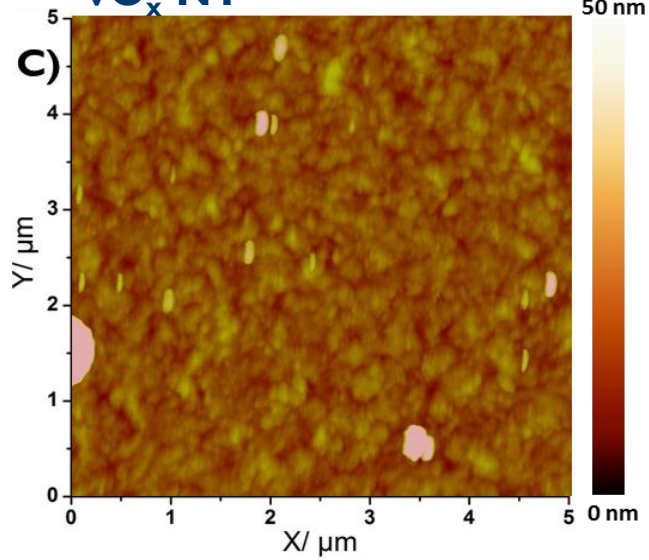

AFM results:

- Films A) and C) showed a quite smooth nanocrystalline surface structure.
- Film B) had an interesting tubular like surface.
- All the films seemed to be polycrystalline.

SPM and SEM characterization:

Film B) V_2O_5 + VO_x-NT

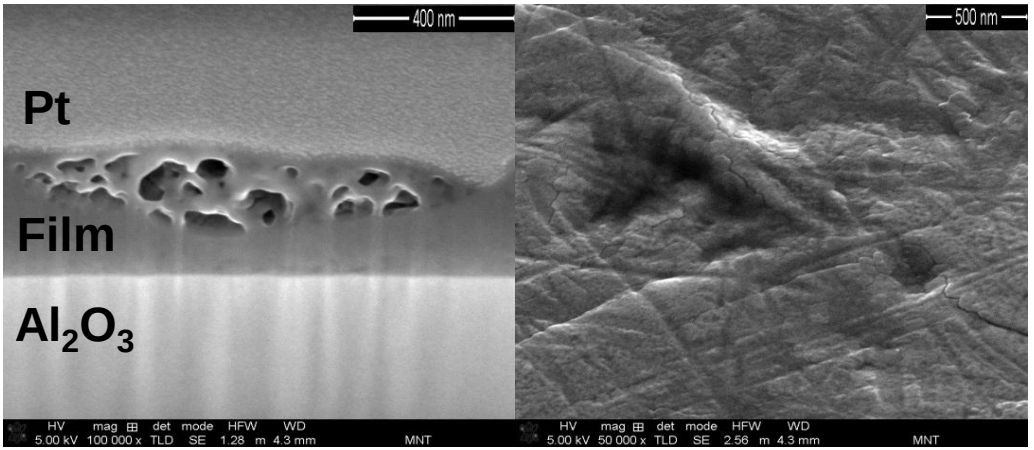

Focused ion beam etching (FIB) was used to make the measurements with SEM!

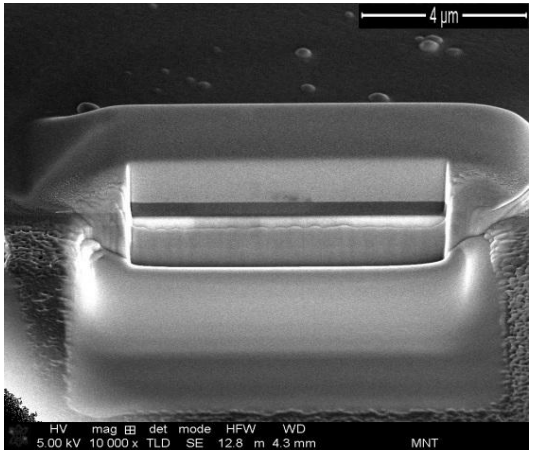

Film C) VO_x-NT

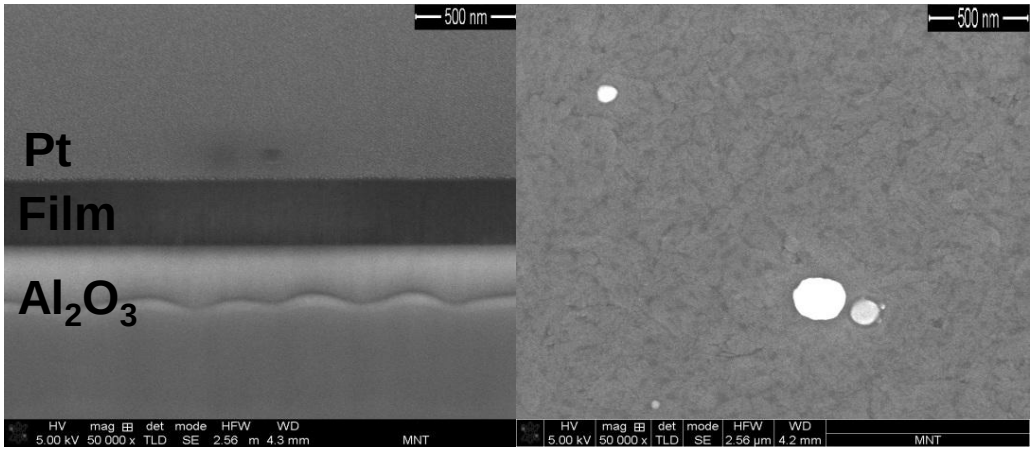

-The V_2O_5 thin film (A) had a quite smooth surface and a polycrystalline structure.
-The V_2O_5 + VO_x-NT mixture phase film (B) had rough surface and a porous, polycrystalline structure (the porosity has an effect on conductivity).
-The VO_x-NT thin film (C) had a smooth surface with a polycrystalline structure.

Optical transmittance characterization:

- Film A) showed a clear transmittance spectrum of V_2O_5 phase.

- As the new phase (VO_x-NT) became stronger in films B) and C), the optical transmittance spectrum also changed accordingly.

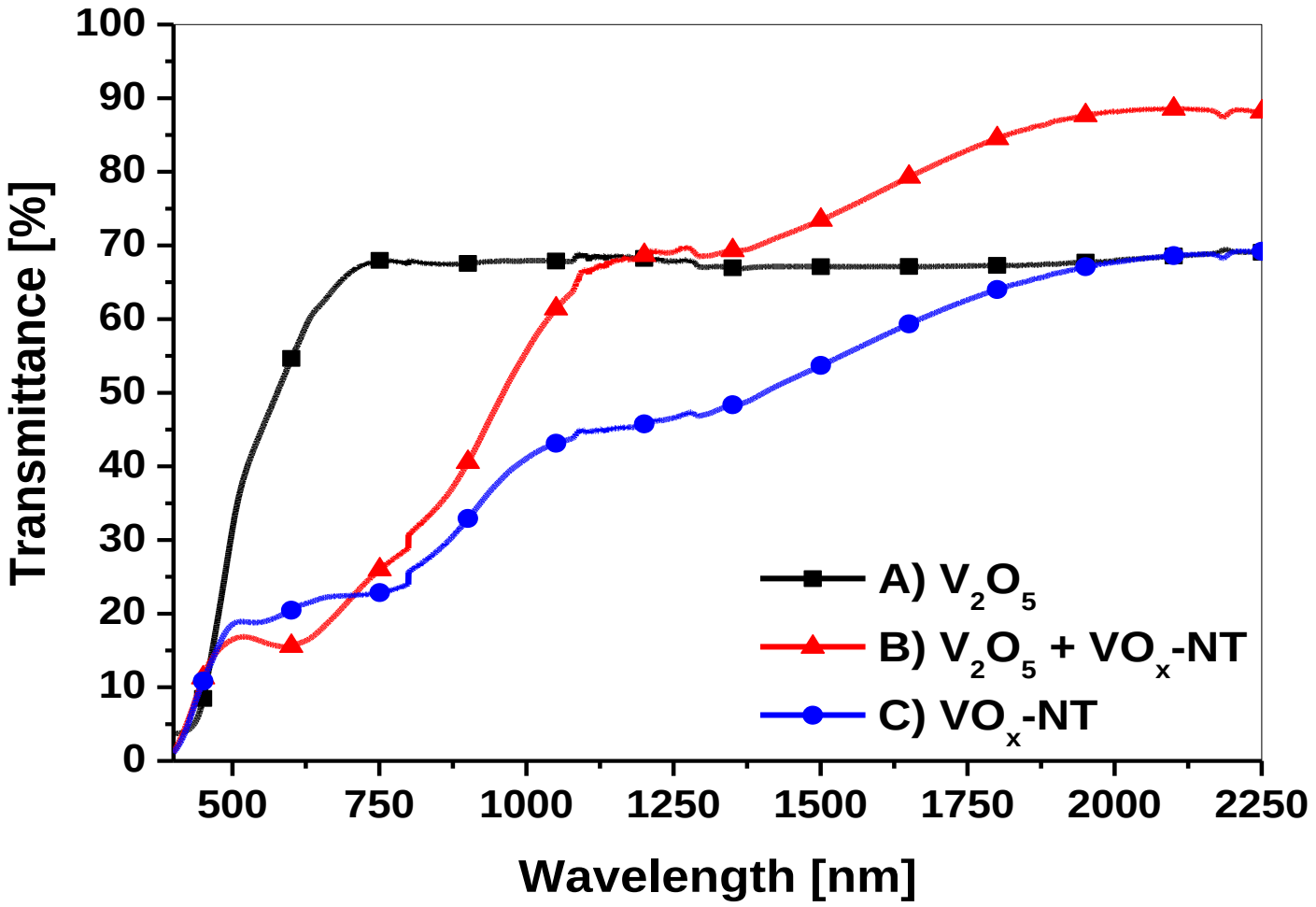

I-V, ρ(T) measurements, and conduction mechanism:

- All the thin films showed a typical semiconducting behaviour.
- The highest value of resistivity was found in film B) and the lowest in film C).
- Insets show the Arrhenius plots of the results: the highest activation energy was found in film B) and the lowest in film C).

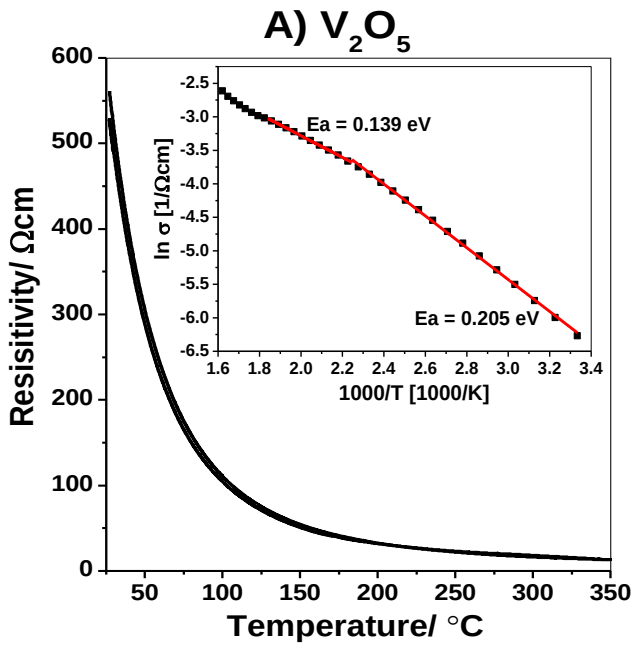

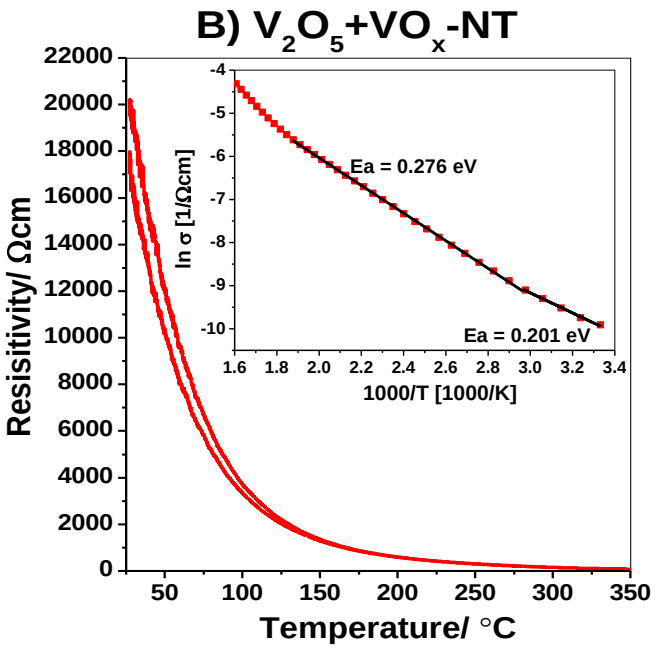

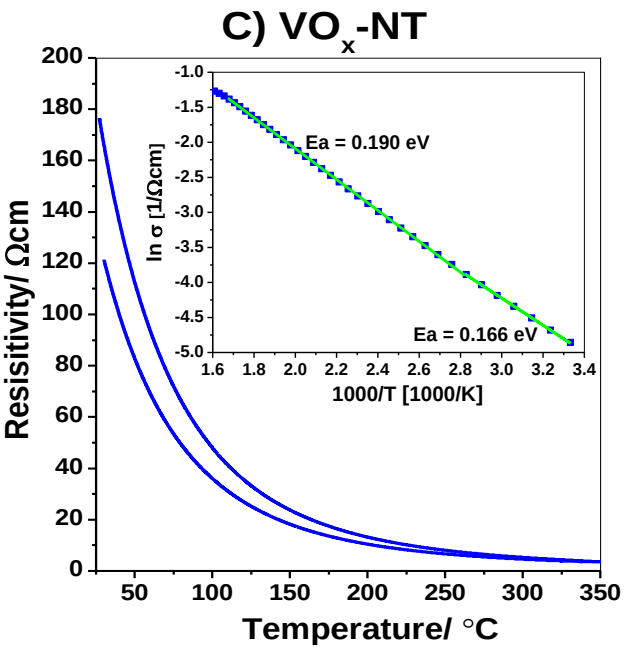

Gas response of the thin films:

NO_x response of the thin films:

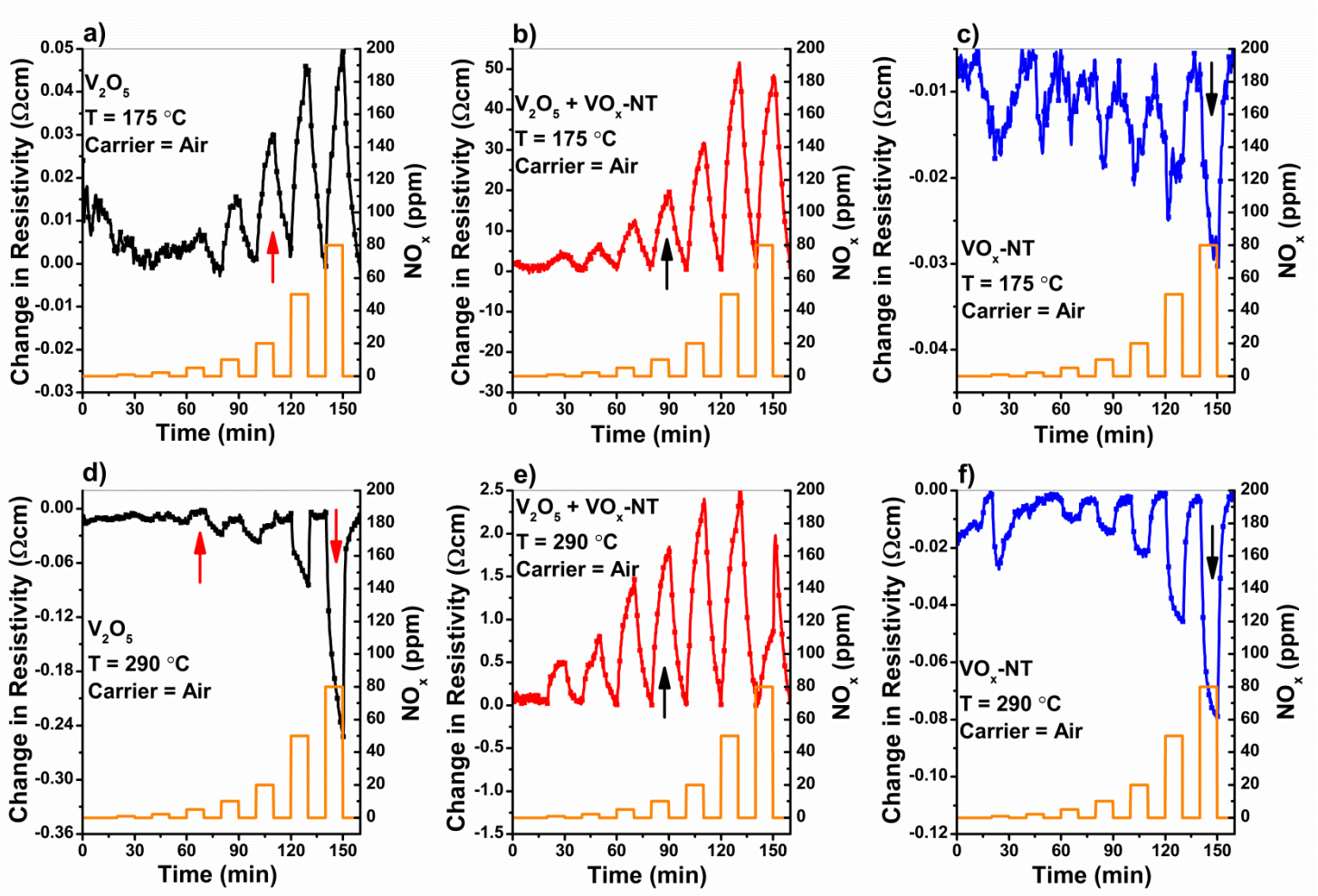

Gas response of the thin films:

H_2 in Air -response of the thin films:

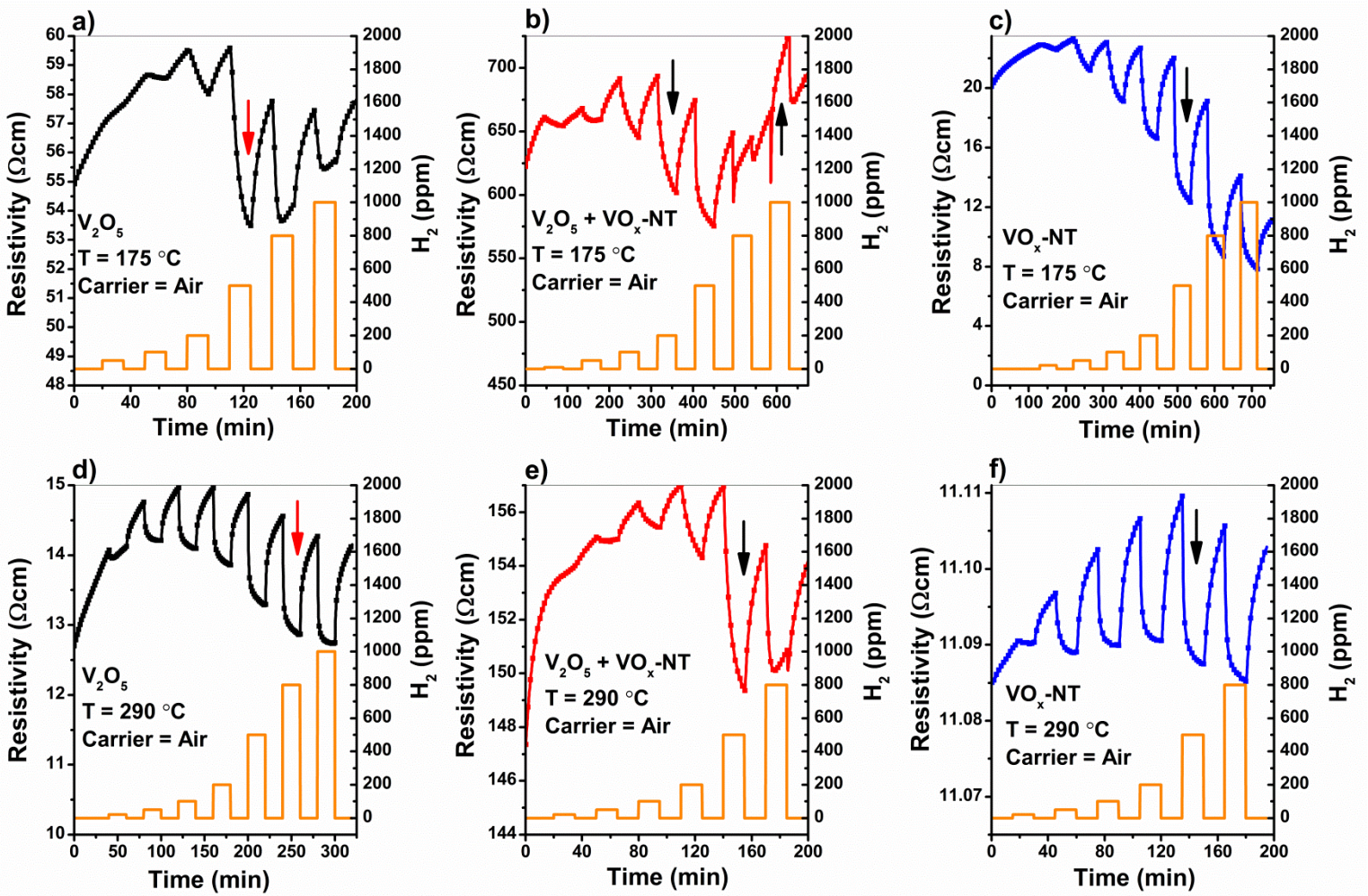

Gas response of the thin films:

H_2 in Argon -response of the thin films:

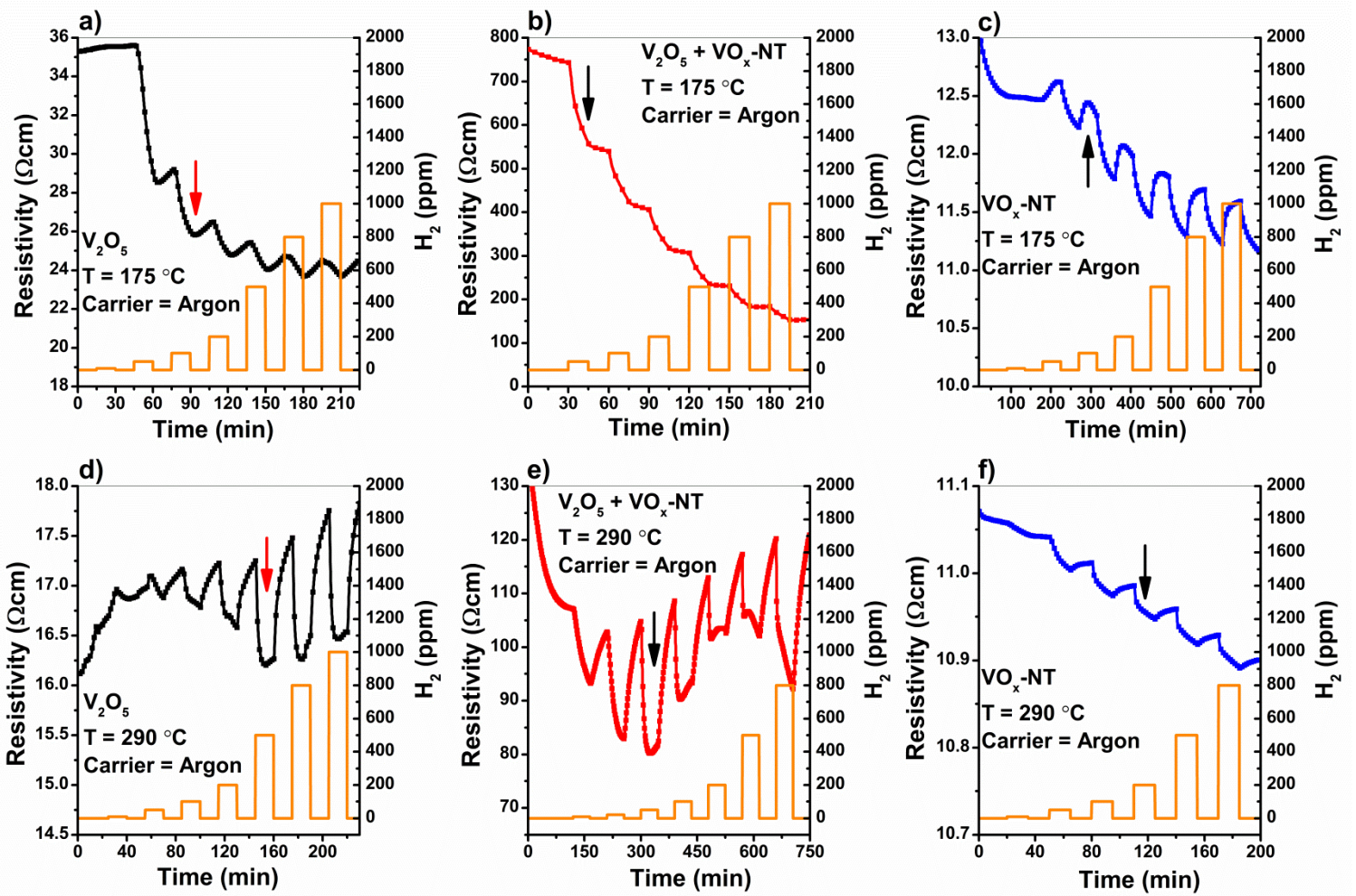

Gas response of the thin films:

Oxygen and H_2 response again – ***p***-type or ***n***-type conductor, or both?

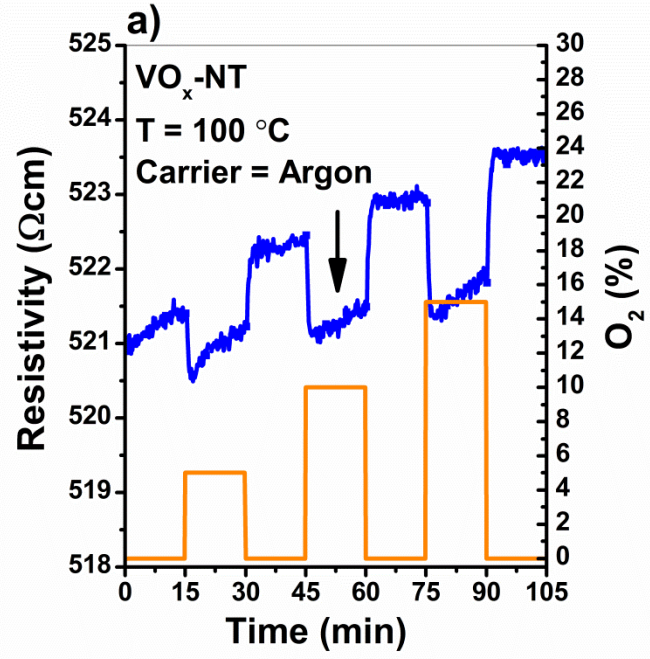

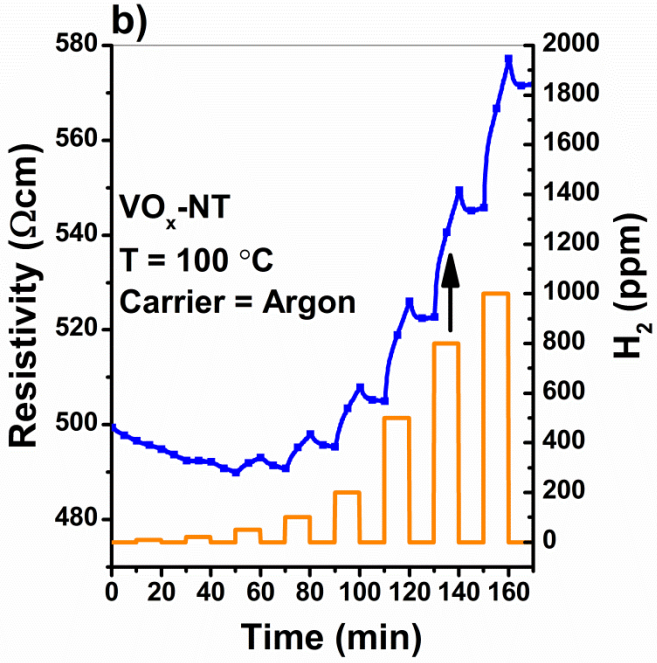

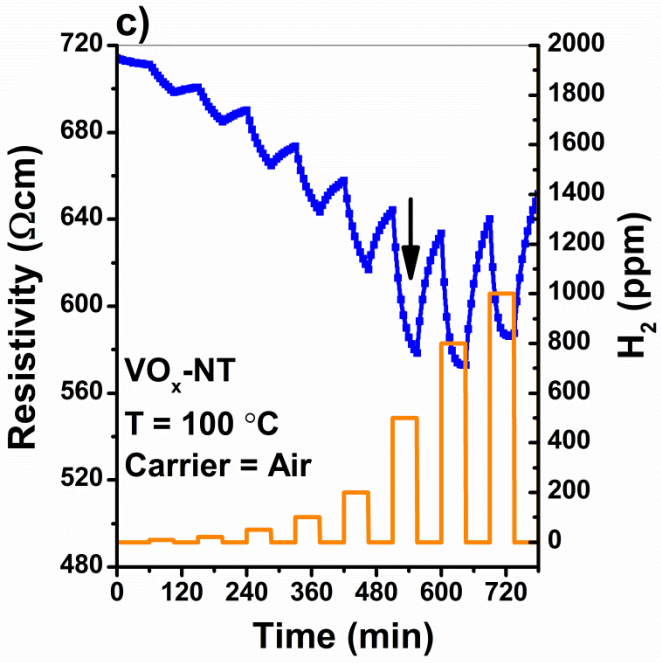

Conclusions:

1. WO_3 nanoparticles and thin films by PLD:
   - Nanoparticles down to f < 40 nm at RT
   - Stable ferroelectric ε-WO_3 phase at RT
   - High H_2S and H_2 response
   - Flipping in NO_x response

2. Inkjet printed metal decorated WO_3 nanoparticle gas sensors:
   - Decoration of WO_3 nanoparticles with metal NP's
   - Cost effecient massproduciton method
   - Extremely high H_2 response

3. Vanadium oxide nanostructures by PLD:
   - Interesting mixed phase of V_2O_5 and V_7O_{16} (VO_x-NT type phase)
   - V_7O_{16} (VO_x-NT type phase) shows *p*-type or *n*-type conduction depending on temperature and atmosphere
   - Mixed phase structure V_2O_5 and V_7O_{16} (VO_x-NT type phase) showed highest response for all studied gases
   - Gas response for ammonia, ethanol, VOC's will be interesting!

Thank you for your attention!